Adaptive Feedforward Compensation Algorithms for Active Vibration Control with Mechanical Coupling and Local Feedback - a unified approach

Ioan Doré Landau, Tudor-Bogdan Airimitoaie, Marouane Alma

▶ **To cite this version:**

Adaptive Feedforward Compensation Algorithms for Active Vibration Control with Mechanical Coupling and Local Feedback - a unified approach

Ioan Doré Landau[a], Tudor-Bogdan Airimiţoaie[a,b], Marouane Alma[a]

[a]*Control System Department of GIPSA-Lab, University of Grenoble, St. Martin d'Héres, 38402 France*
[b]*ACSE Department, University "Politehnica" of Bucharest, Bucharest, 060042 Romania*

Abstract

Adaptive feedforward broadband vibration (or noise) compensation is currently used when a correlated measurement with the disturbance (an image of the disturbance) is available. Most of the active vibration control systems feature an internal "positive" mechanical feedback between the compensation system and the reference source (a correlated measurement with the disturbance). Such systems have often also a feedback control loop for reducing the effect of disturbances. Therefore the adaptive feedforward compensation algorithms should take into account this structure. For stability reasons the adaptation algorithms requires the implementation of a filter on observed data or a filtering of the residual acceleration in order to satisfy some passivity conditions. The paper proposes new algorithms for the adaptive feedforward compensation in this context with both filtering of data and of the residual acceleration and using an "Integral + Proportional" (IP) adaptation as a means for accelerating the transients as well as for relaxing the positive real conditions required by the stability analysis. The paper also shows that the main interest in filtering the residual acceleration is to shape in the frequency domain the power spectral density (PSD) of the residual acceleration. The algorithms have been applied to an active vibration control (AVC) system and real time results illustrating the advantages of the proposed algorithms are presented.

Keywords: active vibration control, adaptive feedforward compensation, RS controller, adaptive control, hybrid feedforward-feedback compensation, parameter estimation

List of acronyms

ANC	Active noise control	IP-PAA	"Integral + proportional" parameter adaptation algorithm
ANVC	Active noise and vibration control		
AVC	Active vibration control	O.D.E.	Ordinary differential equation
EFR	Equivalent feedback representation	PAA	Parameter adaptation algorithm
FIR	Finite impulse response	PRBS	Pseudo random binary sequence
FULMS	Filtered-u least mean squares	PSD	Power spectral density
IIR	Infinite impulse response	SHARF	Simplified hyperstable adaptive recursive filter
IP	"Integral + proportional"	SPR	Strictly positive real (transfer function)

1. Introduction

Adaptive feedforward for broadband disturbance compensation is widely used when a well correlated with the disturbance signal (image of the disturbance) is available ([1–4]). However, in many systems, there

is a positive mechanical coupling between the feedforward compensation system and the measurement of the image of the disturbance. This often leads to the instability of the system.

In the context of this inherent "positive" feedback, the adaptive feedforward compensator should minimize the effect of the disturbance while simultaneously assuring the stability of the internal positive feedback loop.

An approach discussed in the literature is the analysis in this new context of existing algorithms for adaptive feedforward compensation developed for the case without feedback. An attempt is made in [5] where the asymptotic convergence in a stochastic environment of the so called "Filtered-U LMS" (FULMS) algorithm is discussed. Further results on the same direction can be found in [6]. The authors use the Ljung's ODE method ([7]) for the case of a scalar vanishing adaptation gain. Unfortunately this is not enough because nothing is said about the stability of the system with respect to initial conditions and when a non vanishing adaptation gain is used (to keep adaptation capabilities). The authors assume that the positive feedback does not destabilize the system.

A stability approach to develop appropriate adaptive algorithms in the context of internal positive feedback is discussed in [8] and [9]. In [9] there is also an experimental comparison of various algorithms for IIR adaptive compensators in the presence of the internal positive feedback.

Combining adaptive feedforward compensation with feedback control has been considered as an issue to further improve the performance of the adaptive feedforward compensation alone. Several references are available, such as [10–12]. While various procedures for designing the fixed feedback controller can be considered, it is clear that an improvement of the global performance can be obtained. Unfortunately, there is a strong interaction between the presence of this local feedback controller and the stability conditions for the adaptive feedforward compensations algorithms. One of the important observations resulting from the analysis developed in this paper, is that the stability conditions for the adaptive feedforward compensation are highly influenced by the design of the feedback loop. This interaction is further enhanced when the internal positive coupling is present. The major practical consequence is that the filters used in order to assure the stability conditions for the adaptive feedforward compensation will depend upon the elements of the feedback compensation loop built around the secondary path and upon the parameters of the positive internal feedback loop.

Another important issue in adaptive feedforward compensation is the design of filters either on the observed variables of the feedforward compensator or on the residual acceleration in order to satisfy positive realness conditions on some transfer functions. In [9] based on the work done by [13], it was shown that for small adaptation gains (slow adaptation) the violation of the positive real conditions in some frequency regions is acceptable, provided that in the average, the input-output product associated with this transfer function is positive. It is in fact a signal dependent condition.

However, the problem of removing or relaxing the positive real condition can be also approached by adding a proportional adaptation to the widely used integral adaptation. While this approach is known in adaptive control [14, 15], it has not been used apparently in the context of adaptive feedforward compensation. One other effect of the "Integral + Proportional" (IP) adaptation is that of speeding up the transients of the adaptation error.

A subject of debate in the context of adaptive feedforward compensation was the choice between filtering the data or filtering the residual acceleration (error) in order to satisfy the positive realness conditions required by the stability analysis (in the presence of the internal positive feedback or not). Some of the references discussing this issue are [16–19]. As it will be shown, the reason to use one of the two options is related to the criterion which is minimized and to the presence or not of unstable zeros in the secondary path. The filtering of the residual error will affect the PSD of the residual error. There are a number of situ-

ations where shaping the residual error in the frequency domain is very useful. A more detailed discussion on the various implications of both types of filtering will be done later in this paper.

From the user point of view and taking into account the type of operation of adaptive disturbance compensation systems, one has to consider two modes of operation of the adaptive schemes:

- Adaptive operation. The adaptation is performed continuously with a non vanishing adaptation gain and the feedforward compensator is updated at each sampling.

- Self-tuning operation. The adaptation procedure starts either on demand or when the performance is unsatisfactory. A vanishing adaptation gain is used.

Scalar adaptation gains are used in some algorithms for adaptive feedforward compensation, but most of the recent algorithms use RLS type matrix adaptation gains able to cover both self tuning and adaptive operations. In the context of the absence of internal feedback, [17] gives a detailed comparison of the two types of adaptation gain. A quite similar comparison in the presence of the internal positive feedback can be found in [9]. Although not detailed in this paper, it is important to keep in mind that the time varying adaptation gains associated with RLS type algorithms require the use of a UD factorization for implementation in real time in order to avoid numerical errors due to round off errors [14, 20]. The complexity of the algorithms has been one of the reasons why initially algorithms using a scalar adaptation gain have been used. It turns out that using an array type implementation strongly reduces the complexity of algorithms using RLS type matrix adaptation gain. This is very pertinently shown in the context of adaptive feedforward compensation in [21].

The objectives of the paper are:

- To introduce the IP adaptation algorithm for adaptive feedforward compensation;
- To introduce new algorithms allowing simultaneously the filtering of the observation vector and/or the filtering of the residual error;
- To make a stability analysis in the presence of internal positive feedback and local linear feedback;
- To provide the rationale for the choice of various filters used in adaptive feedforward compensation;
- To provide a general form for the adaptive feedforward compensation algorithms which includes as particular cases (almost) all adaptive feedforward IIR compensator algorithms available in the literature.

The main contributions of this paper are:

- Analysis of the interaction between the local feedback loop and the adaptive feedforward compensation in the presence of an internal positive feedback coupling;
- Development and analysis of a general algorithm for adaptive feedforward compensation in the presence of an internal positive coupling and a local feedback controller using both filtering of the observations and of the residual error and an Integral + Proportional Parameter Adaptation Algorithm (IP-PAA);
- Enhancement of the role of the desired performance criterion in the design of specific algorithms;
- Enhancement of the use of proportional adaptation to relax the positive real conditions;
- Comparison of the new algorithms with some existing algorithms;
- Application of the algorithms to an active vibration control system featuring internal positive mechanical coupling.

The paper is organized as follows. The experimental setup is described in Section 2. The system representation and feedforward and feedback compensator structures are given in Section 3. The algorithms for adaptive feedforward compensation are developed in Section 4 and analyzed in Section 6. A discussion of the various algorithms is presented in Section 5. The problem of SPR relaxation is discussed in Section 7. In Section 8, a comparison with other algorithms from the literature is done. Section 9 presents experimental results obtained on the AVC system described in Sectin 2.

2. An Active Vibration Control System Using an Inertial Actuator
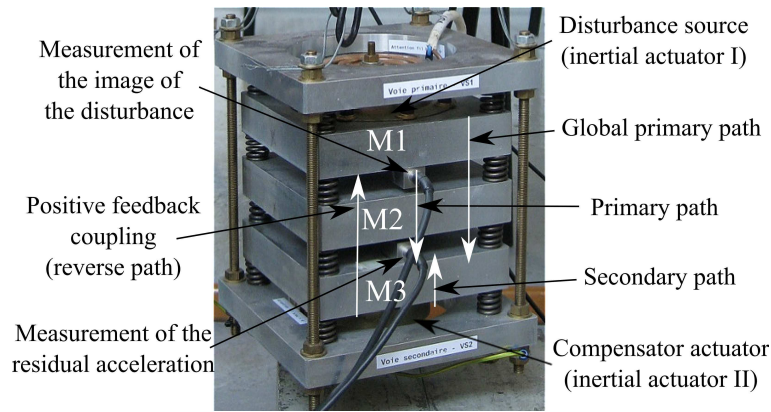

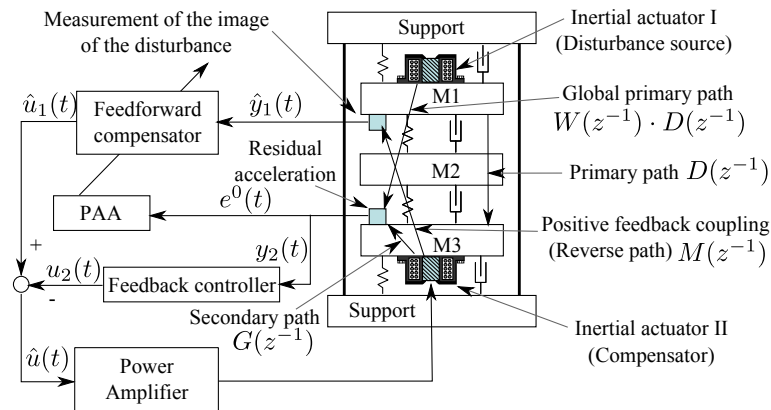Figure 1: The AVC system used for experimentations - photo.

Figure 2: An AVC system using an adaptive feedforward and a fixed feedback compensation scheme.

Figures 1 and 2 represent an AVC system using a measurement correlated with the disturbance and an inertial actuator for reducing the residual acceleration. The structure is representative for a number of situations encountered in practice.

The system consists of 5 metallic plates (in dural of 1.8 Kg each one) connected by springs. The plates M1 and M3 are equipped with inertial actuators. The one on M1 serves as disturbance generator (inertial actuator 1 in Figure 2), the one on M3 serves for disturbance compensation (inertial actuator 2 in Figure 2). The system is equipped with a measure of the residual acceleration (on plate M3) and a measure of the image of the disturbance made by an accelerometer posed on plate M1.
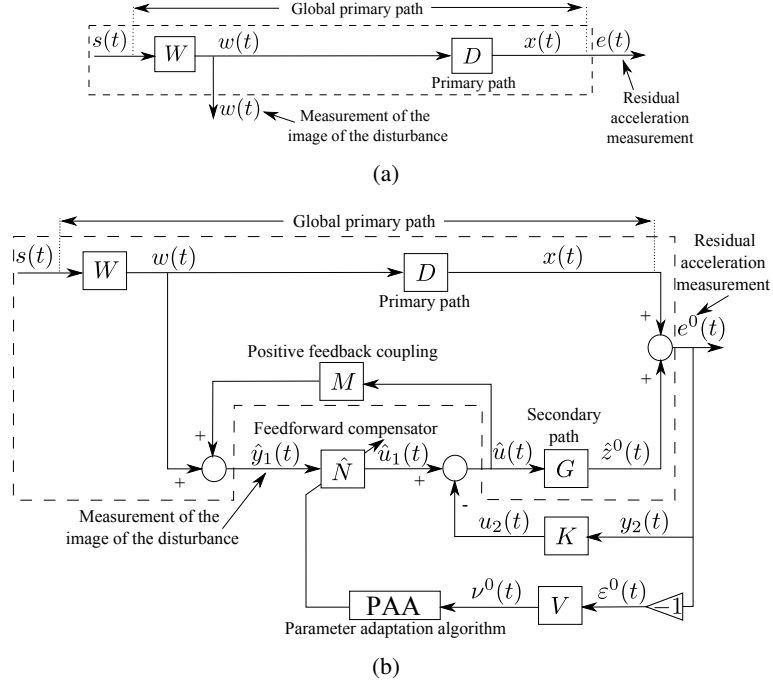
Figure 3: Feedforward AVC: in open loop (a), with RS controller and adaptive feedforward compensator (b).

The path between the disturbance (in this case, generated by the inertial actuator on top of the structure), and the residual acceleration is called the **global primary path**. The path between the measure of the image of the disturbance and the residual acceleration (in open loop) is called the **primary path** and the path between the inertial actuator for compensation and the residual acceleration is called the **secondary path**. When the compensator system is active, the actuator acts upon the residual acceleration, but also upon the measurement of the image of the disturbance (a positive feedback). The measured quantity $\hat{y}_1(t)$ will be the sum of the correlated disturbance measurement $w(t)$ obtained in the absence of the feedforward compensation (see Figure 3(a)) and of the effect of the actuator used for compensation.

The disturbance is the position of the mobile part of the inertial actuator (see Figures 1 and 2) located on top of the structure. The input to the compensator system is the position of the mobile part of the inertial actuator located on the bottom of the structure.

The corresponding block diagrams in open loop operation and with the hybrid (feedback-feedforward) compensation system are shown in Figures 3(a) and 3(b), respectively. In Figure 3(b), $\hat{y}_1(t)$ denotes the effective output provided by the measurement device and which will serve as input to the adaptive feedforward filter $\hat{N}$. The control signal $\hat{u}(t)$, resulting from the difference between the output of the feedforward filter denoted by $\hat{u}_1(t)$ and the output of the feedback controller, is applied to the actuator through an amplifier. The transfer function G (the secondary path) characterizes the dynamics from the control signal to the residual acceleration measurement($e^0(t)$) (amplifier + actuator + dynamics of the mechanical system). The transfer function D between $w(t)$ and the measurement of the residual acceleration (in open loop operation) characterizes the primary path.

The coupling between the control signal $\hat{u}(t)$ and the measurement $\hat{y}_1(t)$ through the compensator actuator is denoted by M. As indicated in Figure 3(b), this coupling is a "positive" feedback. This unwanted coupling raises problems in practice (source of instabilities) and makes the analysis of adaptive (estimation)

5

algorithms more difficult. The system shown in Figure 3(b) can be represented in the standard feedback form shown in Figure 4 (for details see Section 3).
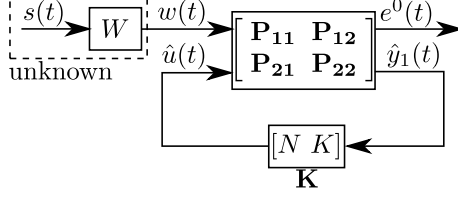

Figure 4: Feedback representation of the system shown in Figure 3(b).

At this stage it is important to mention that very reliable models of the various paths can be obtained by system identification techniques in the absence of the feedforward and feedback filters.

3. Basic Equations and Notations

The different blocks of the AVC system (Figure 3(b)) are described in this section. The primary path is characterized by the asymptotically stable transfer operator

$$D(q^{-1}) = \frac{B_D(q^{-1})}{A_D(q^{-1})}, \tag{1}$$

where[1]

$$B_D(q^{-1}) = b_1^D q^{-1} + ... + b_{n_{B_D}}^D q^{-n_{B_D}} = q^{-1} B_D^*(q^{-1}), \tag{2}$$

$$A_D(q^{-1}) = 1 + a_1^D q^{-1} + ... + a_{n_{A_D}}^D q^{-n_{A_D}}. \tag{3}$$

The unmeasurable value of the output of the primary path (when the compensation is active) is denoted $x(t)$.

The secondary path is characterized by the asymptotically stable transfer operator

$$G(q^{-1}) = \frac{B_G(q^{-1})}{A_G(q^{-1})}, \tag{4}$$

where

$$B_G(q^{-1}) = b_1^G q^{-1} + ... + b_{n_{B_G}}^G q^{-n_{B_G}} = q^{-1} B_G^*(q^{-1}), \tag{5}$$

$$A_G(q^{-1}) = 1 + a_1^G q^{-1} + ... + a_{n_{A_G}}^G q^{-n_{A_G}}. \tag{6}$$

The positive feedback coupling is characterized by the asymptotically stable transfer operator

$$M(q^{-1}) = \frac{B_M(q^{-1})}{A_M(q^{-1})}, \tag{7}$$

where

$$B_M(q^{-1}) = b_1^M q^{-1} + ... + b_{n_{B_M}}^M q^{-n_{B_M}} = q^{-1} B_M^*(q^{-1}), \tag{8}$$

---

[1]Throughout the paper, the notation $X(q^{-1}) = x_0 + q^{-1} X^*(q^{-1})$ will be used. Usually, x_0 will either be 1 or 0.

$$A_M(q^{-1}) = 1 + a_1^M q^{-1} + \dots + a_{n_{A_M}}^M q^{-n_{A_M}}. \tag{9}$$

B_G, B_M, and B_D have a one step discretization delay. The identified models of the secondary path and of the positive feedback coupling are denoted $\hat{G}$ and $\hat{M}$, respectively, and their numerators and denominators $\hat{B}_G$, $\hat{A}_G$, $\hat{B}_M$ and $\hat{A}_M$.

The equations associated with the feedback system representation shown in Figure 4 are:

$$\begin{bmatrix} e^0(t) \\ \hat{y}_1(t) \end{bmatrix} = \begin{bmatrix} \mathbf{P_{11}} & \mathbf{P_{12}} \\ \mathbf{P_{21}} & \mathbf{P_{22}} \end{bmatrix} \begin{bmatrix} w(t) \\ \hat{u}(t) \end{bmatrix} = \begin{bmatrix} D & G \\ 1 & M \end{bmatrix} \begin{bmatrix} w(t) \\ \hat{u}(t) \end{bmatrix}, \tag{10}$$

$$\hat{u}(t) = \mathbf{K}^T \hat{\mathbf{y}}(t), \tag{11}$$

$$\mathbf{K} = [\hat{N}, \ -K]^T, \tag{12}$$

$$\hat{\mathbf{y}}^T(t) = [\hat{y}_1(t), \ y_2(t)] = [\hat{y}_1(t), \ e^0(t)], \tag{13}$$

where $e^0(t)$ is the performance variable to be minimized (residual acceleration), $\hat{y}_1(t)$ is the measured variable (image of the disturbance), $w(t)$ is the disturbance ($w(t) = W(q^{-1})s(t)$), and $\hat{u}(t)$ is the control input[2].

The optimal feedforward filter (unknown) is defined by

$$N(q^{-1}) = \frac{R(q^{-1})}{S(q^{-1})}, \tag{14}$$

where

$$R(q^{-1}) = r_0 + r_1 q^{-1} + \dots + r_{n_R} q^{-n_R}, \tag{15}$$

$$S(q^{-1}) = 1 + s_1 q^{-1} + \dots + s_{n_S} q^{-n_S} = 1 + q^{-1} S^*(q^{-1}). \tag{16}$$

The estimated feedforward filter is denoted by

$$\hat{N}(q^{-1}) = \frac{\hat{R}(q^{-1})}{\hat{S}(q^{-1})}. \tag{17}$$

The vector of optimal feedforward filter parameters is

$$\mathbf{\Theta}^T = [s_1, \ \dots \ s_{n_S}, \ r_0, \ \dots \ r_{n_R}]^T \tag{18}$$

and the vector of estimated feedforward filter parameters is

$$\hat{\mathbf{\Theta}}^T(t) = [\hat{s}_1(t), \ \dots \ \hat{s}_{n_S}(t), \ \hat{r}_0(t), \ \dots \ \hat{r}_{n_R}(t)]^T. \tag{19}$$

The fixed feedback controller K, computed on the basis of the model $\hat{G}$ to reject broadband disturbances on the output $e^0(t)$, is characterized by the asymptotically stable transfer function

$$K(q^{-1}) = \frac{B_K(q^{-1})}{A_K(q^{-1})}, \tag{20}$$

where

$$B_K(q^{-1}) = b_0^K + b_1^K q^{-1} + \dots + b_{n_{B_K}}^K q^{-n_{B_K}}, \tag{21}$$

---

[2]If $w(t)$ is not measured $\mathbf{P_{21}} = 0$. If there is no internal positive coupling $M = 0$.

$$A_K(q^{-1}) = 1 + a_1^K q^{-1} + ... + a_{n_{A_K}}^K q^{-n_{A_K}}. \tag{22}$$

The input of the feedforward filter (called also reference) is denoted by $\hat{y}_1(t)$ and it corresponds to the measurement provided by the primary transducer (force or acceleration transducer in AVC or a microphone in ANC). In the absence of the compensation loop (open loop operation), $\hat{y}_1(t) = w(t)$. The output of the feedforward compensator is denoted by $\hat{u}_1(t+1) = \hat{u}_1(t+1|\hat{\Theta}(t+1))$ (a posteriori output)[3].

The measured input to the feedforward filter can also be written as

$$\hat{y}_1(t+1) = w(t+1) + \frac{B_M^*(q^{-1})}{A_M(q^{-1})}\hat{u}(t), \tag{23}$$

where

$$\hat{u} = \hat{u}_1(t) - u_2(t), \tag{24}$$

$\hat{u}_1(t)$ and $u_2(t)$ are the outputs given by the adaptive feedforward and the fixed feedback compensator, respectively. $\hat{u}$ is the effective input sent to the control actuator.

The a priori output of the estimated feedforward filter is given by

$$\hat{u}_1^0(t+1) = \hat{u}_1(t+1|\hat{\Theta}(t)) = -\hat{S}^*(t,q^{-1})\hat{u}_1(t) + \hat{R}(t,q^{-1})\hat{y}_1(t+1)$$

$$= \hat{\Theta}^T(t)\Phi(t) = \left[\hat{\Theta}_S^T(t), \hat{\Theta}_R^T(t)\right] \begin{bmatrix} \Phi_{\hat{y}_1}(t) \\ \Phi_{\hat{u}_1}(t) \end{bmatrix} \tag{25}$$

where $\hat{\Theta}^T(t)$ has been given in (19) and

$$\Phi^T(t) = [-\hat{u}_1(t), \ \ldots \ -\hat{u}_1(t-n_S+1), \ \hat{y}_1(t+1), \ \hat{y}_1(t), \ \ldots \ \hat{y}_1(t-n_R+1)]$$

$$= [\Phi_{\hat{u}_1}^T(t), \ \Phi_{\hat{y}_1}^T(t)] \tag{26}$$

is called the observation vector.

In the context of this paper, fixed feedback compensators K will be considered. The input to the feedback compensator is given by the performance variable, therefore $y_2(t) = e^0(t)$. Its output will be $u_2(t) = K \cdot y_2(t)$.

The unmeasurable value of the output of the primary path (when the compensation is active) is denoted $x(t)$. The a priori output of the secondary path is denoted $\hat{z}^0(t+1) = \hat{z}(t+1|\hat{\Theta}(t))$ while its input is $\hat{u}(t)$. One has

$$\hat{z}^0(t+1) = \frac{B_G^*(q^{-1})}{A_G(q^{-1})}\hat{u}(t) = \frac{B_G^*(q^{-1})}{A_G(q^{-1})}\hat{u}(t|\hat{\Theta}(t)). \tag{27}$$

The measured residual acceleration (or force) satisfies the following equation

$$e^0(t+1) = x(t+1) + \hat{z}^0(t+1). \tag{28}$$

The filtered a priori adaptation error is defined as

$$\nu^0(t+1) = \nu(t+1|\hat{\Theta}(t)) \tag{29}$$

$$= \varepsilon^0(t+1) + \sum_{i=1}^{n_1} v_i^B \varepsilon(t+1-i) - \sum_{i=1}^{n_2} v_i^A \nu^0(t+1-i), \tag{30}$$

---

[3]In adaptive control and estimation the predicted output at $t+1$ can be computed either on the basis of the previous parameter estimates (a priori, time t) or on the basis of the current parameter estimates (a posteriori, time $t+1$).

where

$$\varepsilon^0(t+1) = \varepsilon(t+1|\hat{\boldsymbol{\Theta}}(t)) = -e^0(t+1) = -x(t+1) - \hat{z}^0(t+1) \tag{31}$$

and

$$\varepsilon(t+1) = \varepsilon(t+1|\hat{\boldsymbol{\Theta}}(t+1)) = -e(t+1) = -x(t+1) - \hat{z}(t+1) \tag{32}$$

are also called, respectively, the a priori and the a posteriori unfiltered adaptation errors.

The coefficients v_i^X, $X \in \{B, A\}$, are the coefficients of an IIR filter, with all poles and zeros inside the unit circle, acting on the adaptation error

$$V(q^{-1}) = \frac{B_V(q^{-1})}{A_V(q^{-1})}, \tag{33}$$

where

$$X_V(q^{-1}) = 1 + q^{-1}X_V^*(q^{-1}) = 1 + \sum_{i=1}^{n_j} v_i^X q^{-i}, \ X \in \{B, A\}. \tag{34}$$

The filtered a posteriori unmeasurable (but computable) adaptation error is given by

$$\nu(t+1) = \nu(t+1|\hat{\boldsymbol{\Theta}}(t+1)) = \varepsilon(t+1) + \sum_{i=1}^{n_1} v_i^B \varepsilon(t+1-i) - \sum_{i=1}^{n_2} v_i^A \nu(t+1-i), \tag{35}$$

with $\varepsilon(t+1)$ given in (32).

The a posteriori value of the output of the secondary path $\hat{z}(t+1)$ (dummy variable) is given by

$$\hat{z}(t+1) = \hat{z}(t+1|\hat{\boldsymbol{\Theta}}(t+1)) = \frac{B_G^*(q^{-1})}{A_G(q^{-1})}\hat{u}(t|\hat{\boldsymbol{\Theta}}(t+1)). \tag{36}$$

For compensators with constant parameters: $\nu^0(t) = \nu(t)$, $\varepsilon^0(t) = \varepsilon(t)$, $e^0(t) = e(t)$, $\hat{z}^0(t) = \hat{z}(t)$, $\hat{u}^0(t) = \hat{u}(t)$.

Remark: when $V(q^{-1}) = 1$ (the adaptation error is not filtered) the a priori and the a posteriori adaptation errors will have respectively the forms

$$\nu^0(t+1) = \nu(t+1|\hat{\boldsymbol{\Theta}}(t)) = \varepsilon(t+1|\hat{\boldsymbol{\Theta}}(t)) = -e^0(t+1) = -x(t+1) - \hat{z}^0(t+1) \tag{37}$$

and

$$\nu(t+1) = \nu(t+1|\hat{\boldsymbol{\Theta}}(t+1)) = \varepsilon(t+1|\hat{\boldsymbol{\Theta}}(t+1)) = -e(t+1) = -x(t+1) - \hat{z}(t+1). \tag{38}$$

4. Development of the Algorithms

The algorithms for adaptive feedforward compensation in the presence of a feedback controller will be developed under the following hypotheses:

H1) The signal $w(t)$ is bounded, i.e.,

$$|w(t)| \le \alpha, \quad \forall t \quad (0 \le \alpha < \infty) \tag{39}$$

(which is equivalent to say that $s(t)$ is bounded and $W(q^{-1})$ in Figure 3 is asymptotically stable).

H2) Perfect matching condition - There exists a filter $N(q^{-1})$ of finite dimension such that

$$\frac{N(z^{-1})}{1 - N(z^{-1})M(z^{-1})}G(z^{-1}) = -D(z^{-1}) \tag{40}$$

and the characteristic polynomials:

- of the "internal" positive coupling loop

$$P(z^{-1}) = A_M(z^{-1})S(z^{-1}) - B_M(z^{-1})R(z^{-1}), \tag{41}$$

- of the closed loop (G-K)

$$P_{cl}(z^{-1}) = A_G(z^{-1})A_K(z^{-1}) + B_G(z^{-1})B_K(z^{-1}), \tag{42}$$

- and of the coupled feedforward-feedback loop

$$P_{fb-ff} = A_M S[A_G A_K + B_G B_K] - B_M R A_K A_G \tag{43}$$

are Hurwitz.

H3) Deterministic context - The effect of the measurement noise upon the measured residual error is neglected.

H4) The primary path model $D(z^{-1})$ is unknown and constant.

Once the algorithms are developed under these hypotheses, H2 and H3 will be removed and the algorithms will be analyzed in this modified context.

A first step in the development of the algorithms is to establish a relation between the errors on the estimation of the parameters of the feedforward filter (with respect to the optimal values) and the measured unfiltered adaptation error $\epsilon(t+1)$. This is summarized in the following lemma.

Lemma 1. *Let the system be described by eqs.* (1) - (36). *Under hypotheses H1, H2, H3, and H4, using a feedforward compensator $\hat{N}$ with constant parameters, one has:*

$$\varepsilon(t+1|\hat{\Theta}) = \frac{A_M(q^{-1})A_G(q^{-1})A_K(q^{-1})G(q^{-1})}{P_{fb-ff}(q^{-1})}\left[\Theta - \hat{\Theta}\right]^T \Phi(t), \tag{44}$$

where Θ (the vector of parameters of the optimal filter N assuring perfect matching) is given by (18),

$$\hat{\Theta}^T = [\hat{s}_1, \, ... \, \hat{s}_{n_S}, \, \hat{r}_0 \, ... \, \hat{r}_{n_R}] = \left[\hat{\Theta}_S^T, \, \hat{\Theta}_R^T\right] \tag{45}$$

is the vector of constant estimated parameters of $\hat{N}$, and $\Phi(t)$ has been defined in (26).

The proof is this lemma has been given in [22][4]. The results of Lemma 1 can be easily particularized to the case without internal positive feedback or without a feedback controller.

Filtering the vector $\Phi(t)$ with an asymptotically stable filter $L(q^{-1}) = \frac{B_L}{A_L}$, eq. (44) for $\hat{\Theta} = constant$ leads to

$$\varepsilon(t+1|\hat{\Theta}) = \frac{A_M(q^{-1})A_G(q^{-1})A_K(q^{-1})G(q^{-1})}{P_{fb-ff}(q^{-1})L(q^{-1})}\left[\Theta - \hat{\Theta}\right]^T \Phi_f(t) \tag{46}$$

---

[4]However, one should take into account that a change of notations has been done with respect to [22]. The following enumeration gives the correspondance in notation between the present article and [22]: $w(t) \leftrightarrow d(t)$, $\hat{u}_1(t) \leftrightarrow \hat{y}_1(t)$, $\hat{u}(t) \leftrightarrow \hat{y}(t)$, $\hat{y}_1(t) \leftrightarrow \hat{u}(t)$, and $e^0(t) \leftrightarrow \chi^0(t)$.

with

$$\mathbf{\Phi}_f(t) = L(q^{-1})\mathbf{\Phi}(t) \tag{47}$$

and filtering $\varepsilon(t + 1|\hat{\mathbf{\Theta}})$ through the filter $V(q^{-1})$ one gets

$$\nu(t+1|\hat{\mathbf{\Theta}}) = \frac{A_M(q^{-1})A_G(q^{-1})A_K(q^{-1})G(q^{-1})V(q^{-1})}{P_{fb-ff}(q^{-1})L(q^{-1})}\left[\mathbf{\Theta} - \hat{\mathbf{\Theta}}\right]^T \mathbf{\Phi}_f(t). \tag{48}$$

Eq. (48) will be used to develop the adaptation algorithms, neglecting for the moment the non-commutativity of the operators when $\hat{\mathbf{\Theta}}$ is time varying (however an exact algorithm can be derived in such cases - see [14]). Replacing the fixed estimated parameters by the current estimated parameters, eq. (46) becomes the equation of the a posteriori residual filtered adaptation error $\nu(t + 1)$ (which is computed)

$$\nu(t+1) = \frac{A_M(q^{-1})A_G(q^{-1})A_K(q^{-1})V(q^{-1})}{P_{fb-ff}(q^{-1})L(q^{-1})}G(q^{-1})\left[\mathbf{\Theta} - \hat{\mathbf{\Theta}}(t+1)\right]^T \mathbf{\Phi}_f(t). \tag{49}$$

Eq. (49) has the standard form for an a posteriori adaptation error ([14]), which suggests to use the following IP-PAA:

$$\hat{\mathbf{\Theta}}_{\mathbf{I}}(t+1) = \hat{\mathbf{\Theta}}_{\mathbf{I}}(t) + \xi(t)\mathbf{F}_{\mathbf{I}}(t)\mathbf{\Psi}(t)\nu(t+1), \tag{50a}$$

$$\hat{\mathbf{\Theta}}_{\mathbf{P}}(t+1) = \mathbf{F}_{\mathbf{P}}(t)\mathbf{\Psi}(t)\nu(t+1), \tag{50b}$$

$$\varepsilon(t+1) = \frac{\varepsilon^0(t+1)}{1 + \mathbf{\Psi}^T(t)(\xi(t)\mathbf{F}_{\mathbf{I}}(t) + \mathbf{F}_{\mathbf{P}}(t))\mathbf{\Psi}(t)}, \tag{50c}$$

$$\nu(t+1) = \varepsilon(t+1) + \sum_{i=1}^{n_1} v_i^B \varepsilon(t+1-i) - \sum_{i=1}^{n_2} v_i^A \nu(t+1-i), \tag{50d}$$

$$\mathbf{F}_{\mathbf{I}}(t+1) = \frac{1}{\lambda_1(t)}\left[\mathbf{F}_{\mathbf{I}}(t) - \frac{\mathbf{F}_{\mathbf{I}}(t)\mathbf{\Psi}(t)\mathbf{\Psi}^T(t)\mathbf{F}_{\mathbf{I}}(t)}{\frac{\lambda_1(t)}{\lambda_2(t)} + \mathbf{\Psi}^T(t)\mathbf{F}_{\mathbf{I}}(t)\mathbf{\Psi}(t)}\right], \tag{50e}$$

$$\mathbf{F}_{\mathbf{P}}(t) = \alpha(t)\mathbf{F}_{\mathbf{I}}(t), \ \mathbf{F}_{\mathbf{I}}(0) = \gamma(0)\cdot\mathbf{I}, \ \alpha(t) > -0.5, \tag{50f}$$

$$\mathbf{F}(t) = \xi(t)\mathbf{F}_{\mathbf{I}}(t) + \mathbf{F}_{\mathbf{P}}(t) \tag{50g}$$

$$\xi(t) = 1 + \frac{\lambda_2(t)}{\lambda_1(t)}\mathbf{\Psi}^T(t)\mathbf{F}_{\mathbf{P}}(t)\mathbf{\Psi}(t), \tag{50h}$$

$$\hat{\mathbf{\Theta}}(t+1) = \hat{\mathbf{\Theta}}_{\mathbf{I}}(t+1) + \hat{\mathbf{\Theta}}_{\mathbf{P}}(t+1), \tag{50i}$$

$$1 \geq \lambda_1(t) > 0, \ 0 \leq \lambda_2(t) < 2, \ \mathbf{F}_{\mathbf{I}}(0) > 0, \tag{50j}$$

$$\mathbf{\Psi}(t) = \mathbf{\Phi}_f(t), \tag{50k}$$

where $\nu(t + 1)$ is the generalized filtered adaptation error (see also Section 3 for more details), $\lambda_1(t)$ and $\lambda_2(t)$ allow to obtain various profiles for the matrix adaptation gain $\mathbf{F}(t)$ ([14]), and $\gamma(0)$ is a positive scalar value. By taking $\lambda_2(t) \equiv 0$ one obtains a constant adaptation gain matrix and choosing $\mathbf{F}_{\mathbf{I}} = \gamma\mathbf{I}, \gamma > 0$ one gets a scalar adaptation gain). For $\alpha(t) \equiv 0$, one obtains the algorithm with integral adaptation gain introduced in [9].

For the adaptive operation, a $\mathbf{F}_{\mathbf{I}}(t)$ with constant trace can be obtained by automatically computing $\lambda_1(t)$ and $\lambda_2(t)$ at each sampling period as a function of the newly computed trace of the "Integral" adaptation matrix, $\text{tr}(\mathbf{F}_{\mathbf{I}}(t))$, and the desired constant trace, $\text{tr}(\mathbf{F}_{I_0})$. In this case, a design parameter $\alpha_F = \frac{\lambda_1(t)}{\lambda_2(t)}$

(chosen equal to 1 in Section 9) is also used. The equations are given below:

$$\lambda_1(t) = \frac{\text{tr}(\mathbf{F_I}(t))}{\text{tr}(\mathbf{F}_{I_0})}, \quad \lambda_2(t) = \frac{\lambda_1(t)}{\alpha_F}. \tag{51}$$

Note also that eq. (50e) is obtained from

$$\mathbf{F_I}^{-1}(t+1) = \lambda_1(t)\mathbf{F_I}^{-1}(t) + \lambda_2(t)\mathbf{\Psi}(t)\mathbf{\Psi}^T(t), \tag{52}$$

using the matrix inversion lemma ([14]).

5. Discussion of the algorithms

There are a number of major choices:

- "Integral" or "Integral + Proportional" adaptation;
- Matrix or Scalar adaptation gain;
- Constant or Time Varying adaptation gain;
- Filtering of the regressor vector or of the residual error (or both);
- Type of filter.

Some reasons to use one or another choice are given bellow (they result from the analysis of the algorithms which will be detailed in the subsequent sections):

- IP adaptation offers, in general, improved transients and leads to a relaxation of SPR conditions for stability;
- In general time varying matrix adaptation gains offer better results than constant scalar adaptation gain. However, it requires significantly more computer power;
- Filtering of the observation vector is in our opinion the best choice for assuring the SPR stability conditions;
- Filtering of the residual error allows to introduce a frequency weighting on the criterion to be minimized;
- Filtering of the residual error can be used also for satisfying the SPR condition but only if the secondary path has stable zeros (in the example considered in this paper the secondary path has unstable zeros). However, this will introduce a frequency weighting in the criterium to be minimized not necessarily coherent with the objectives.

In Table 1, several versions of the algorithms particularized for various choices of V and L are given. In the last line of Table 1,

$$\hat{P}_{fb-ff} = \hat{A}_M \hat{S} \left[\hat{A}_G A_K + \hat{B}_G B_K \right] - \hat{B}_M \hat{R} A_K \hat{A}_G \tag{53}$$

is an estimation of the characteristic polynomial of the coupled feedforward-feedback loop computed on the basis of available estimates of the parameters of the filter $\hat{N}$.

For the Algorithms III, several options for updating $\hat{P}_{fb-ff}$ can be considered:

- Run one of the Algorithms I or II for a certain time to get estimates of $\hat{R}$ and $\hat{S}$;
- Run a simulation (using the identified models);
- Update $\hat{P}_{fb-ff}$ at each sampling instant or from time to time using Algorithm III (after a short initialization horizon using one of the Algorithms I or II).

12

Regressor filtering		Error filtering		Double filtering	
Alg.	Filter L ($V = 1$)	Alg.	Filter V ($L = 1$)	Alg.	Filters (V and L)
I_L	$L = \hat{G}$	I_V	$V = \frac{1}{\hat{G}}$	I_{LV}	$L = \hat{G}, \; V \neq 1$
II_L	$L = \frac{\hat{G}}{1+\hat{G}K}$	II_V	$V = \frac{1+\hat{G}K}{\hat{G}}$	II_{LV}	$L = \frac{\hat{G}}{1+\hat{G}K}, \; V \neq 1$
III_L	$L = \frac{\hat{A}_M \hat{A}_G A_K}{\hat{P}_{fb-ff}} \hat{G}$	III_V	$V = \frac{\hat{P}_{fb-ff}}{\hat{A}_M \hat{A}_G A_K \hat{G}}$	III_{LV}	$L = \frac{\hat{A}_M \hat{A}_G A_K}{\hat{P}_{fb-ff}} \hat{G}, \; V \neq 1$

Table 1: Adaptation algorithms with regressor vector and/or residual error filtering.

6. Analysis of the Algorithms

6.1. Deterministic case

The equation for the a posteriori adaptation error has the form

$$\nu(t+1) = H(q^{-1})\left[\boldsymbol{\Theta} - \hat{\boldsymbol{\Theta}}(t+1)\right]^T \boldsymbol{\Psi}(t) \tag{54}$$

where

$$H(q^{-1}) = \frac{A_M A_G A_K}{P_{fb-ff}}\frac{GV}{L}, \; \boldsymbol{\Psi} = \boldsymbol{\Phi}_f. \tag{55}$$

Neglecting the non-commutativity of the time varying operators, one has the following result

Theorem 1. *Assuming that eq. (54) represents the evolution of the a posteriori adaptation error and that the IP-PAA (50) is used, one has:*

$$\lim_{t\to\infty} \nu(t+1) = 0 \tag{56}$$

$$\lim_{t\to\infty} \frac{[\nu^0(t+1)]^2}{1 + \boldsymbol{\Psi}(t)^T \mathbf{F}(t)\boldsymbol{\Psi}(t)} = 0 \tag{57}$$

$$||\boldsymbol{\Psi}(t)|| \text{ is bounded} \tag{58}$$

$$\lim_{t\to\infty} \nu^0(t+1) = 0 \tag{59}$$

for any bounded initial conditions $\hat{\boldsymbol{\Theta}}(0)$, $\nu^0(0)$, $\mathbf{F}(0)$, provided that

$$H'(z^{-1}) = H(z^{-1}) - \frac{\lambda_2}{2}, \; \max_t \lambda_2(t) \leq \lambda_2 < 2, \; \forall t \tag{60}$$

is a SPR transfer function.

The proof[5] of (56) is given in Appendix A. For (57), (58), and (59), the proof follows [9, 23] and is omitted.

It should be observed that the PAA with "Integral + Proportional" adaptation gain presented here, is a generalization of that given in Theorem 3.2 of [9]. Note also that $\mathbf{P}(t)$, $\mathbf{Q}(t)$, $\mathbf{S}(t)$, and $\mathbf{R}(t)$ used in the proof of Appendix A are generalized forms of those used in the proof of the theorem mentioned above for "Integral" PAA.

---

[5] $\nu^0(t+1)$ is computed using $\hat{\boldsymbol{\Theta}}(t) = \hat{\boldsymbol{\Theta}}_{\mathbf{I}}(t)$.

The proof of [24] for IP adaptation with time varying integral adaptation gain is given for $\xi(t) = \frac{1}{\lambda_1(t)} + \frac{\lambda_2(t)}{\lambda_1(t)} \mathbf{\Psi}^T(t)\mathbf{F_P}(t)\mathbf{\Psi}(t)$. To the knowledge of the authors, the proof for $\xi(t) = 1 + \frac{\lambda_2(t)}{\lambda_1(t)} \mathbf{\Psi}^T(t)\mathbf{F_P}(t)\mathbf{\Psi}(t)$ is presented here for the first time.

Remark: Consider eq. (49) with $V(q^{-1}) = 1$. Neglecting the non-commutativity of time varying operators it can be written as

$$\nu(t+1) = [\mathbf{\Theta} - \hat{\mathbf{\Theta}}(t+1)]^T \mathbf{\Phi}'_f(t), \tag{61}$$

$$\mathbf{\Phi}'_f(t) = \frac{A_M(q^{-1})A_G(q^{-1})A_K(q^{-1})G(q^{-1})}{P_{fb-ff}(q^{-1})} \mathbf{\Phi}(t). \tag{62}$$

If one would like to minimize a one step ahead quadratic criterion

$$J(t+1) = \nu^2(t+1) \tag{63}$$

using the gradient technique [14], one gets

$$\frac{1}{2}\frac{\partial J(t+1)}{\partial \hat{\mathbf{\Theta}}(t+1)} = -\mathbf{\Phi}'_f(t)\nu(t+1). \tag{64}$$

Using Algorithm III_L, eq. (50a) can be viewed as an approximation of the gradient ($\mathbf{F} = \gamma\mathbf{I} = const$, $\alpha(t) = 0$, $\xi(t) = 1$, for the gradient technique). For constant adaptation gain, $\lambda_2(t) \equiv 0$ and the strict positive realness on $H'(z^{-1})$ implies at all the frequencies

$$-90^0 < \angle\frac{A_M(\mathrm{e}^{-j\omega})B_G(\mathrm{e}^{-j\omega})A_K(\mathrm{e}^{-j\omega})}{P_{fb-ff}(\mathrm{e}^{-j\omega})} - \angle\frac{\hat{A}_M(\mathrm{e}^{-j\omega})\hat{B}_G(\mathrm{e}^{-j\omega})A_K(\mathrm{e}^{-j\omega})}{\hat{P}_{fb-ff}(\mathrm{e}^{-j\omega})} < 90^0. \tag{65}$$

Therefore the interpretation of the SPR condition of Theorem 1 is that the angle between the direction of adaptation and the direction of the inverse of the true gradient should be less than 90^0. For time-varying adaptation gains the condition is sharper since in this case $\mathrm{Re}\{H(\mathrm{e}^{-j\omega})\}$ should be larger than $\frac{\lambda}{2}$ at all frequencies.

Remark: Algorithms III allow almost always to satisfy the SPR condition provided that good estimations of M and G are available.

6.2. Effect of the measurement noise (The stochastic case - perfect matching)

The details of the analysis in this context is given in Appendix B. The conclusion is that in the presence of measurement noise, provided that one uses a decreasing adaptation gain, convergence of the parameters towards the optimal ones with probability 1 is assured under the same SPR conditions as in the deterministic case (provided that a wide band disturbance is acting on the system).

6.3. The case of non-perfect matching

If $\hat{N}(t, q^{-1})$ does not have the appropriate dimension, there is no chance to satisfy the perfect matching condition. Two problems are of interest in this case:

1. The boundedness of the residual error
2. The bias distribution in the frequency domain

6.3.1. Boundedness of the residual error

Results from [25, 26] can be used to analyze the boundedness of the residual error. The following assumptions are made:

1. There exists a reduced order filter $\hat{N}$, characterized by the unknown polynomials $\hat{S}$ (of order n_S) and $\hat{R}$ (of order n_R), for which the polynomials given in eqs. (41)-(43), where S and R have been replaced by $\hat{S}$ and $\hat{R}$, are Hurwitz.

2. The output of the optimal filter satisfying the matching condition can be expressed as

$$\hat{u}_1(t+1) = -\left[\hat{S}^*(q^{-1})\hat{u}_1(t) - \hat{R}(q^{-1})\hat{y}_1(t+1) + \eta(t+1)\right], \tag{66}$$

where $\eta(t+1)$ is a norm bounded signal.

Using the results of [25, Theorem 4.1, pp. 1505-1506] and assuming that $w(t)$ is norm bounded, it can be shown that all the signals are norm bounded under the passivity condition (60), where $\hat{P}_{fb-ff}$ is computed now with the reduced order estimated filter.

6.3.2. Bias distribution

Using the Parseval's relation, the asymptotic bias distribution of the estimated parameters in the frequency domain can be obtained, starting from the expression of $\nu(t)$, by taking into account that the algorithm minimizes (almost) a criterion of the form $\lim_{N\to\infty} \frac{1}{N}\sum_{t=1}^{N} \nu^2(t)$.

The bias distribution (for Algorithm III_{LV}), taking into account eq. (40) is given by

$$\hat{\boldsymbol{\Theta}}^* = \arg\min_{\hat{\boldsymbol{\Theta}}} \int_{-\pi}^{\pi} \left|V(\mathrm{e}^{-j\omega})\right|^2 \cdot \left[\left|S_{NM}(\mathrm{e}^{-j\omega})\right|^2 \left|N(\mathrm{e}^{-j\omega}) - \hat{N}(\mathrm{e}^{-j\omega})\right|^2 \cdot\right.$$

$$\left. \cdot \left|\frac{1}{1 - \hat{N}(\mathrm{e}^{-j\omega})M(\mathrm{e}^{-j\omega}) + K(\mathrm{e}^{-j\omega})G(\mathrm{e}^{-j\omega})}\right|^2 \left|G(\mathrm{e}^{-j\omega})\right|^2 \boldsymbol{\Phi}_w(\omega) + \boldsymbol{\Phi}_n(\omega)\right] \mathrm{d}\omega \tag{67}$$

where $S_{NM} = \frac{1}{1-NM}$ is the output sensitivity function of the internal closed loop for the optimal controller and $\boldsymbol{\Phi}_w(\omega)$ and $\boldsymbol{\Phi}_n(\omega)$ are the spectral densities of the disturbance and measurement noise.

From (67) one concludes that a good approximation of $N(q^{-1})$ will be obtained in the frequency region where $\boldsymbol{\Phi}_w$ is significant and where $G(q^{-1})$ has a high gain (usually $G(q^{-1})$ should have high gain in the frequency region where $\boldsymbol{\Phi}_w$ is significant in order to counteract the effect of $w(t)$). However, the quality of the estimated $\hat{N}(q^{-1})$ will be affected also by the output sensitivity function of the internal closed loop $N - M$. Clearly, the introduction of the filter $V(q^{-1})$ on the adaptation error will shape the frequency distribution of the error.

7. Relaxing the Positive Real Condition

7.1. Averaging theory for the relaxation of the SPR condition

It is possible to relax the SPR conditions taking into account that:

1. The disturbance (input to the system) is a broadband signal;
2. Most of the adaptation algorithms work with a low adaptation gain.

Under these two assumptions, the behavior of the algorithm can be well described by the "averaging theory" developed in [7, 13] (see also [14]). When using the averaging approach, the basic assumption of a slow adaptation holds for small adaptation gains (constant and scalar in [13], i.e., $\lambda_2(t) \equiv 0, \lambda_1(t) = 1$; matrix and time decreasing asymptotically in [7, 14], i.e., $\lim_{t \to \infty} \lambda_1(t) = 1, \lambda_2(t) = \lambda_2 > 0$ or scalar and time decreasing).

In the context of averaging, the basic condition for stability is that

$$\lim_{N \to \infty} \frac{1}{N} \sum_{t=1}^{N} \mathbf{\Phi}(t) H'(q^{-1}) \mathbf{\Phi}^T(t) = \frac{1}{2} \int_{-\pi}^{\pi} \mathbf{\Phi}(e^{j\omega})[H'(e^{j\omega}) + H'(e^{-j\omega})]\mathbf{\Phi}^T(e^{-j\omega})d\omega > 0 \qquad (68)$$

be a positive definite matrix ($\mathbf{\Phi}(e^{j\omega})$ is the Fourier transform of $\mathbf{\Phi}(t)$).

One can view (68) as the weighted energy of the observation vector $\mathbf{\Phi}$. Of course the SPR sufficient condition upon $H'(z^{-1})$ (see eq. (60)) allows to satisfy this condition. However in the averaging context it is only needed that (68) is true which allows that H' be non positive real in a limited frequency band (for more details see [9]). This explains why Algorithms I and II will work in practice in most of the cases. While the stability of the system can be guaranteed the performance may be not very good. In this paper, another approach for the relaxation of the SPR condition is given, which can be used especially in the initialisation stages (when using Algorithms I or II). The motivation for this is provided in the following subsection.

7.2. Relaxing the positive real condition by IP adaptation

The adaptive system formed by eq. (54) and the adaptation algorithm (50) admits an equivalent feedback representation (EFR) for $\lambda_1(t) \equiv 1, \lambda_2(t) \equiv 0$ (constant adaptation gain). The stability condition of eq. (60) (in this case $H'(z^{-1}) = H(z^{-1})$) is a direct consequence of the passivity of the equivalent feedback path, since if the feedback path is passive, it is enough that the equivalent linear feedforward path is SPR (see [14]). However, this condition is only sufficient. There is an additional "excess" of passivity in the feedback path (which depends upon the adaptation gains and on the magnitude of $\mathbf{\Psi}(t)$) which can be transferred to the linear feedforward block in order to relax the SPR condition. This idea was prompted out in the context of recursive identification by Tomizuka and results have been given for the case of integral adaptation and for the case when the equivalent linear feedforward path is characterized by an all poles (no zeros) transfer function (see [15]). These results have been extended in [14] for "Integral + Proportional" adaptation with constant adaptation gain.

In what follows, the results of [14, 15] will be extended to the case of linear equivalent feedforward paths characterized by a poles-zeros transfer function and taking into account the presence of the proportional adaptation which increases significantly the reserve of passivity of the equivalent feedback path.

Theorem 2. *The adaptive system described by eq. (54) and eqs. (50) for $\lambda_2(t) \equiv 0$ and $\lambda_1(t) \equiv 1$ is asymptotically stable provided that:*

T1) *There exists a gain K such that $\frac{H}{1+KH}$ is SPR,*

T2) *The adaptation gains $\mathbf{F_I}$ and $\mathbf{F_P}(t)$ and the observation vector $\mathbf{\Psi}(t)$ satisfy either*

$$\sum_{t=0}^{t_1} \left[\mathbf{\Psi}^T(t-1) \left(\frac{1}{2}\mathbf{F_I} + \mathbf{F_P}(t-1) \right) \mathbf{\Psi}(t-1) - K \right] \nu^2(t) \geq 0 \qquad (69)$$

for all $t_1 \geq 0$ or

$$\mathbf{\Psi}^T(t) \left(\frac{1}{2}\mathbf{F_I} + \mathbf{F_P}(t) \right) \mathbf{\Psi}(t) > K > 0, \qquad (70)$$

16

Reference	Adaptation		Adaptation gain		Filtering		Taking into account	
	IP	I	Matrix	Scalar	Regressor vector	Residual error	Local feedback	Internal feedback
Present paper	yes	yes	yes	yes	yes	yes	yes	yes
[9]	no	yes	yes	yes	yes	no	no	yes
[22]	no	yes	yes	yes	yes	no	yes	yes
[8]	no	yes	no	yes	no	no	no	yes
FULMS	no	yes	no	yes	yes	no	no	yes
SHARF [16]	no	yes	no	yes	no	yes	no	no
[17]	no	yes	yes	no	yes	yes	no	no

Table 2: Comparison of algorithms for adaptive feedforward compensation in AVC with mechanical coupling.

for all $t \geq 0$.

The proof of this theorem is given in Appendix C.

8. Comparison with Other Algorithms

The IP adaptation in the context of adaptive feedforward compensation is introduced for the first time the present paper. Only algorithms dedicated to IIR feedforward compensators will be considered. Algorithms dedicated to FIR feedforward compensators are a special case of those dedicated to IIR compensator and will not be discussed here.

The algorithms introduced in this paper are compared with the algorithms presented in [9], [8], [17], the FULMS ([5]), and the SHARF ([16]). Table 2 gives a synthetic comparison. Detailed comparison can be done using Tables D.3 and D.4 from Appendix D, where all the algorithms are summarized.

9. Experimental Results

9.1. Objective of the experiments

The experiments considered in this paper concern the system described in Section 2. For the case of "Integral" adaptation and in the presence of internal feedback, reference [9] provides extensive experimental evaluation of the algorithms and comparison with other "Integral" algorithms considered in [5] and [8]. The benefit of adding local feedback is studied theoretically and experimentally in [22]. The objectives of the experiments to be presented in this paper are to illustrate (i) the advantages of using IP adaptation and (ii) the rationale for using filtering on the regressor and/or the filtering on the residual error (these are the two major novelties of this paper).

9.2. System identification

The experiments are conducted on a system with internal positive feedback and with or without local feedback. A detailed view of the mechanical structure used for the experiments has been given in Figure 1. The methodology used for parametric identification of the mechanical structure's paths is similar to that of [9, 26, 27]. The sampling frequency is 800 Hz.

The secondary and reverse paths have been identified in the absence of the feedforward compensator (see Figure 3(b)) using as excitation signal a PRBS generated by a 10 bit shift register and a frequency
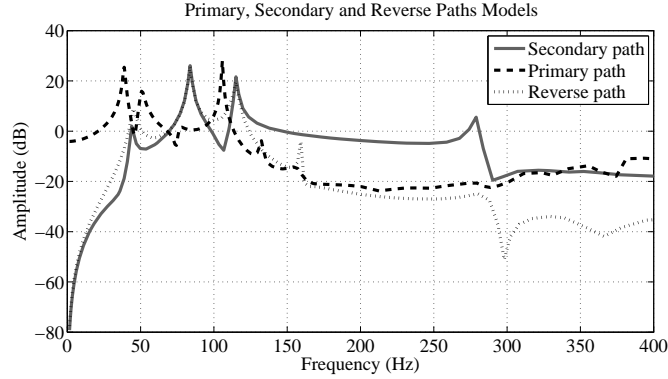
Figure 5: Frequency characteristics of the primary, secondary and reverse paths

divider $p = 4$ applied at the input of the amplifier feeding the inertial actuator used for compensation[6] (see Figures 1 and 2). For the secondary path, $G(q^{-1})$, the output is the residual acceleration measurement, $e(t)$. For the reverse path, $M(q^{-1})$, the output is the signal delivered by the primary transducer (accelerometer) $\hat{y}(t)$.

The estimated orders of the model for the secondary path are $n_{B_G} = 14$, $n_{A_G} = 14$. The best results, in terms of validation, have been obtained with the **Recursive Extended Least Square** method. The frequency characteristic of the secondary path is shown in Figure 5, solid line. It features several very low damped vibration modes. The first vibration mode is at 44 Hz with a damping of 0.0212, the second at 83.8 Hz with a damping of 0.00961, the third one at 115 Hz with a damping of 0.00694. There is also a pair of low damped complex zeros at 108 Hz with a damping of 0.021. As a consequence of the double differentiator behavior, a double zero at $z = 1$ is also present.

For the reverse path $M(q^{-1})$, the model's complexity has been estimated to be $n_{B_M} = 13$, $n_{A_M} = 13$. The frequency characteristic of the reverse path is shown in Figure 5 (dotted line). There are several very low damped vibration modes at 45.1 Hz with a damping of 0.0331, at 83.6 Hz with a damping of 0.00967, at 115 Hz with a damping of 0.0107 and some additional modes in high frequencies. There are two zeros on the unit circle corresponding to the double differentiator behavior. The gain of the reverse path is of the same order of magnitude as the gain of the secondary path up to 150 Hz, indicating a strong feedback in this frequency zone.

The primary path has been identified in the absence of the feedforward compensator using $w(t)$ as an input and measuring $e(t)$. The disturbance $s(t)$ was a PRBS sequence (N=10, frequency divider p=2). The estimated orders of the model are $n_{B_D} = 26$, $n_{A_D} = 26$. The frequency characteristic is presented in Figure 5 (dashed line) and may serve for simulations and detailed performance evaluation. Note that the primary path features a strong resonance at 108 Hz, exactly where the secondary path has a pair of low damped complex zeros (almost no gain). Therefore one can not expect good attenuation around this frequency.

9.3. Design of the feedback controller

The objective of the feedback RS controller K is to reduce the disturbance effect on the residual acceleration ($e^0(t)$) where the secondary path G has enough gain and without using the correlated measurement

---

[6]It was first verified with $p = 2$ that there are no significant dynamics around 200 Hz and then $p = 4$ has been chosen in order to enhance the power spectral density of the excitation in low frequencies while keeping a reasonable length for the experiment.

$\hat{y}_1(t)$. To do this, the problem has been formulated as an H_∞ problem by using the appropriate weighting functions. This minimization problem has been solved using pole placement with sensitivity function shaping techniques presented in [28], by following these steps

- The poles of the negative feedback loop formed by the secondary path and the controller K have been selected as those of the open loop (poles of G) with the observation that the poles at 83.8 Hz and 115 Hz have been damped to 0.1 and 0.02 respectively;
- The loop has been opened in low and high frequencies by choosing $H_R(q^{-1}) = (1 + q^{-1})(1 - q^{-1})$ as a fixed part of the controller numerator;
- 15 real auxiliary robustness poles, at 0.3, have been added such that: $n_{P_{cl}} \le n_{A_G} + n_{B_G} + n_{H_R} + n_{H_S} + d - 1 = 29$.

Figure 6 shows the performance of the feedback controller with respect to the open loop. A 13 dB of global attenuation is obtained.

9.4. *Broadband disturbance rejection with feedback controller and various filtering*

The adaptive feedforward filter structure for all of the experiments has been $n_R = 3$, $n_S = 4$ (total of 8 parameters). This complexity does not allow to verify the "perfect matching condition" (not enough parameters). A PRBS excitation on the global primary path will be considered as the disturbance.

Several experiments have been conducted allowing to understand the effects of the various choices:

- I adaptation with filtering of the regressor;
- IP adaptation with filtering of the regressor;
- IP adaptation with filtering of the regressor and of the adaptation error.

For the adaptive operation[7] the Algorithms I_L and I_{LV} have been used with scalar adaptation gain ($\lambda_1(t) = 1$, $\lambda_2(t) = 0$)[8]. The experiments have been carried out by first applying the disturbance in open loop during 50 sec and after that, closing the loop with the adaptive feedforward algorithms in the presence of the fixed feedback controller. The experiments have been run over a 1500 sec time period.

Time domain results obtained on the AVC system with only an "Integral" PAA are shown in Figure 7. Figure 8 shows the time domain result obtained using the IP-PAA. The advantage of using an IP-PAA is an overall improvement of the transient behavior. A variable $\alpha(t)$ in the PAA has been chosen, starting with an initial value of 200 and linearly decreasing to 100 (over a horizon of 25 sec).

In Figure 9, in addition to the IP-PAA a filtering of the adaptation error using $V(q^{-1}) = 1 - 0.9q^{-1}$ has been introduced, using Algorithm I_{LV} (which introduces a weight in high frequencies). In this case, $\alpha(t)$ has been initialized at 200 and was linearly decreased to 10 over a horizon of 950 sec.

A comparison of the PSDs obtained with the three adaptive algorithms is presented in Figure 10. One observes an improvement of the attenuation given by the IP-PAA algorithm with adaptation error filtering and no degradation with respect to the open loop in high frequencies, which is coherent with the $V(q^{-1})$ filter that has been used. It has to be mentioned that for the PSDs only the last ten seconds of the 1500 sec experiments have been taken into account.

It is clear that "Integral + Proportional" adaptation gives better results than only "Integral" adaptation and that using a filtering of the adaptation error can also have a good effect.

---

[7] Algorithms I_V - III_V can not be used in our case since the secondary path has unstable zeros.

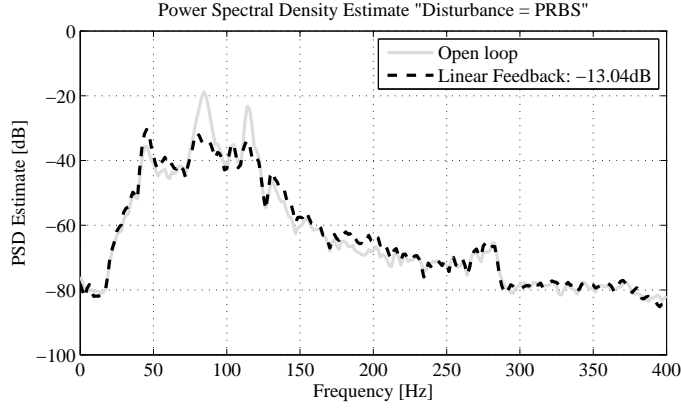[8] Note that Algorithm I_L uses the same filtering as the FuLMS algorithm.

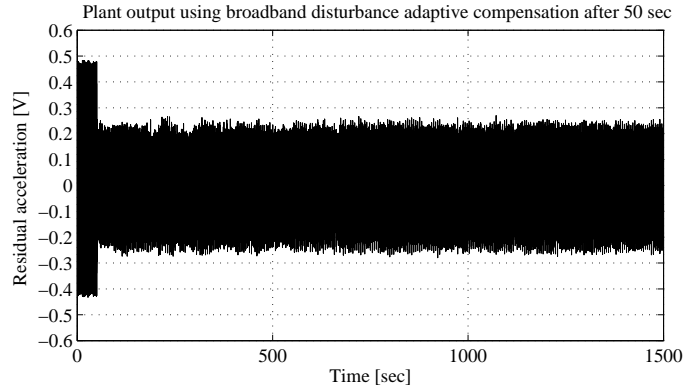Figure 6: Power spectral density of the open loop and when using the fixed feedback controller.

Figure 7: Real time results obtained with Algorithm I_L using "Integral" scalar adaptation gain.

9.5. Broadband disturbance rejection using only the feedforward adaptive filter

As it turns out, in the hybrid case, the positive real condition was satisfied even with Algorithm I_L in the frequency region from 0 to 300 Hz, which under the slow adaptation gain assumption is enough to guarantee the stability of the system taking also into consideration the frequency characteristics of the disturbance (Figure 10, open loop). In this subsection, the case without fixed feedback compensator is considered. The objective is to show that the SPR condition can be relaxed in a more general case when this is an issue.

In the absence of the feedback controller, $B_K(q^{-1}) = 0$ and $A_K(q^{-1}) = 1$, and with no filtering of the adaptation error, $V(q^{-1}) = 1$, eq. (55) for Algorithm I_L becomes

$$H(q^{-1}) = \frac{A_M G}{P\hat{G}}. \tag{71}$$

The advantage of using an IP-PAA is an overall improvement of the transient behavior despite the fact that the SPR condition on $H(q^{-1})$ is not satisfied as shown in Figure 11 (the SPR condition is not satisfied around 83 Hz and around 116 Hz). Note that Figure 11 corresponds to an estimation of this transfer function assuming $\hat{G} = G$, $\hat{M} = M$ and $P = A_M\hat{S} - B_M\hat{R}$ in which the parameters of $\hat{R}$ and $\hat{S}$ have been obtained by running the adaptation algorithm for 1500 sec. A variable $\alpha(t)$ in the PAA has been chosen, starting
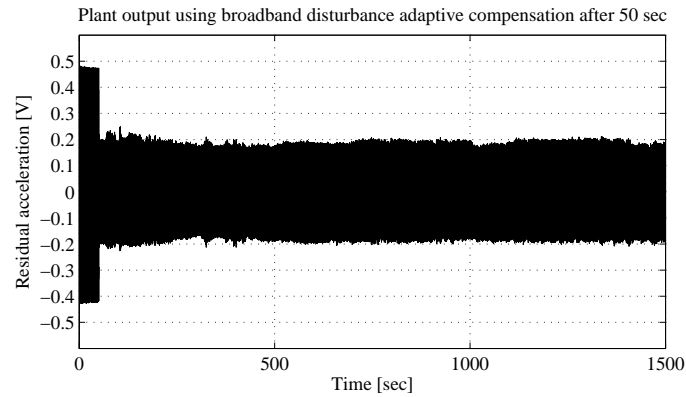
20

Figure 8: Real time results obtained with Algorithm I_L using "Integral + Proportional" scalar adaptation gain.
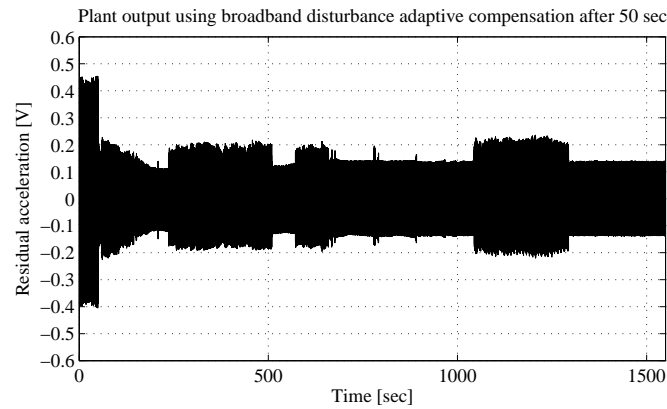

Figure 9: Real time results obtained with Algorithm I_{LV} using "Integral + Proportional" scalar adaptation gain and adaptation error filtering.

with an initial value of 200 and linearly decreasing to 100 (over a horizon of 25 sec). The most important objective has been to improve the performance during the initial transient period, thus a large value for $\alpha(t)$ has been used at start decreasing to smaller values so that parameter variations could be reduced in the end, thus obtaining better global attenuations.

Figure 12 shows the comparison between I and IP adaptation over an horizon of 1500 sec. Figure 13 is a zoom of Figure 12 covering only the first 30 sec after the introduction of the adaptive feedforward compensator. It is clear that IP adaptation gives better results on a long run. The effect in the initial phase of the adaptation, Figure 13, is an acceleration of transients. It can be observed that the adaptation error is limited, to the interval $[-0.3, 0.3]$, 10 sec faster when using IP-PAA than when using basic integral adaptation.

10. Conclusions

The paper has considered the situation occurring in adaptive feedforward compensation when there exists a positive internal feedback coupling and a feedback controller. The introduction of a feedback controller on one hand modifies the stability conditions and on the other hand can improves significantly the performances of the adaptive feedforward compensation schemes. The paper has considered algorithms
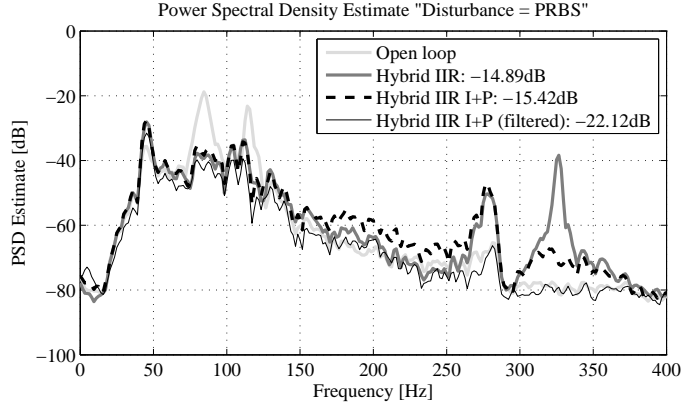
21

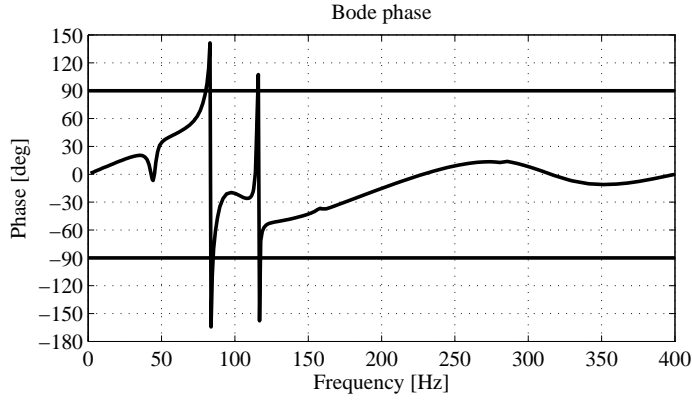Figure 10: Power spectral density of the adaptive filters.

Figure 11: Phase of estimated $H(z^{-1})$ for Algorithm I_L.

which simultaneously use filtering of the regressor vector (used in the adaptation algorithm) and filtering of the residual error (adaptation error). It was shown and verified experimentally that the filters on the residual error can be used for shaping the PSD of the residual error. The paper has introduced integral+ proportional adaptation algorithms in the context of the adaptive feedforward compensation, which allow to relax the positive real conditions for stability and improve the performance. Most of the algorithms used in adaptive feedforward compensation appear as particular case of the algorithms introduced in this paper.

Appendix A. Proof of the A Posteriori Adaptation Error's Asymptotic Stability in Theorem 1

Proof. From eqs. (50) and (54), one can obtain the equivalent feedback representation (EFR) described by:
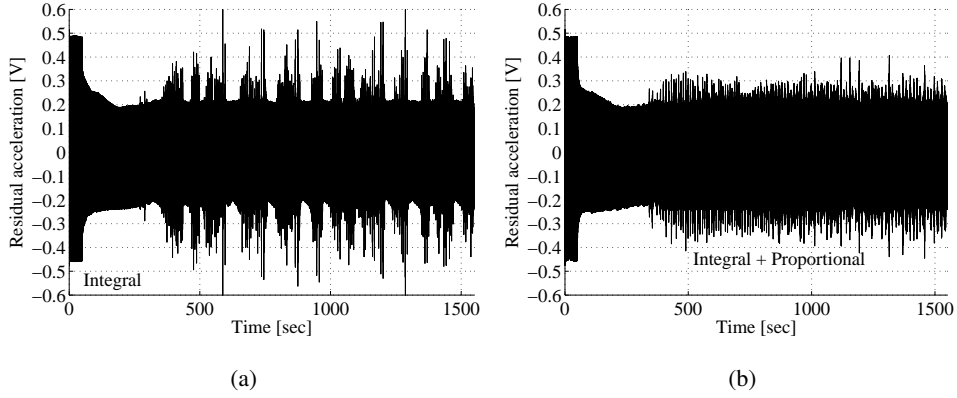
Figure 12: Real time results obtained with Algorithm I_L using (a) "Integral" scalar adaptation gain and (b) "Integral + Proportional" scalar adaptation gain over 1500 sec.
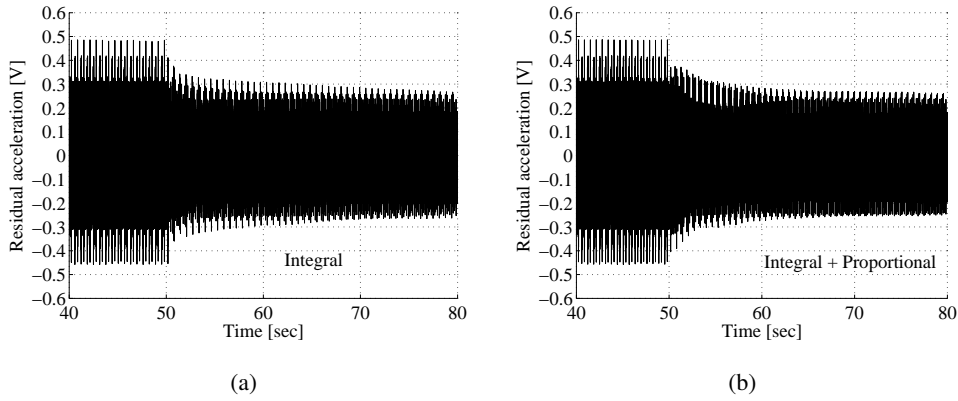

Figure 13: Real time results obtained with Algorithm I_L using (a) "Integral" scalar adaptation gain and (b) "Integral + Proportional" scalar adaptation gain.

$$\nu(t+1) = -\left(H(z^{-1}) - \frac{\lambda_2}{2}\right)\bar{y}_{e2}(t) \tag{A.1}$$

$$\tilde{\boldsymbol{\Theta}}_{\mathbf{I}}(t) = \hat{\boldsymbol{\Theta}}_{\mathbf{I}}(t) - \boldsymbol{\Theta}, \tag{A.2}$$

$$\tilde{\boldsymbol{\Theta}}_{\mathbf{I}}(t+1) = \tilde{\boldsymbol{\Theta}}_{\mathbf{I}}(t) + \xi(t)\mathbf{F}_{\mathbf{I}}(t)\boldsymbol{\Psi}(t)\left(\nu(t+1) - \frac{\lambda_2}{2}\bar{y}_{e2}(t)\right), \tag{A.3}$$

$$\bar{y}_{e2}(t) = \boldsymbol{\Psi}^T(t)\tilde{\boldsymbol{\Theta}}_{\mathbf{I}}(t) + \boldsymbol{\Psi}^T(t)\mathbf{F}(t)\boldsymbol{\Psi}(t)\left(\nu(t+1) - \frac{\lambda_2}{2}\bar{y}_{e2}(t)\right), \tag{A.4}$$

The feedforward path (eq. (A.1)) is characterized by a SPR transfer function (see eq. (60)). It can be shown, using the results of [24], that the equivalent feedback path described by eqs. (A.3) and (A.4) satisfies the Popov inequality (passive block). For this we need the results [24, Theorem 1] and [24, Lemma 2].

23

Considering the following change of notations:

$$\mathbf{A}(t) = \mathbf{I}, \ \mathbf{B}(t) = \xi(t)\mathbf{F_I}(t)\boldsymbol{\Psi}(t), \ \mathbf{C}(t) = \boldsymbol{\Psi}^T(t), \ D(t) = \boldsymbol{\Psi}^T(t)\mathbf{F}(t)\boldsymbol{\Psi}(t), \tag{A.5}$$

it can be sown that the equivalent feedback path is passive, i.e., one satisfies [24, Lemma 2], by choosing:

$$\mathbf{P}(t) = \mathbf{F_I}^{-1}(t), \tag{A.6}$$

$$\mathbf{Q}(t) = [1 - \lambda_1(t)]\mathbf{F_I}^{-1}(t), \tag{A.7}$$

$$\mathbf{S}(t) = [1 - \lambda_1(t)]\boldsymbol{\Psi}(t), \tag{A.8}$$

$$f_{\mathbf{F_I}}(t) \stackrel{\text{def}}{=} \boldsymbol{\Psi}^T(t)\mathbf{F_I}(t)\boldsymbol{\Psi}(t), \ f_{\mathbf{F_P}}(t) \stackrel{\text{def}}{=} \boldsymbol{\Psi}^T(t)\mathbf{F_P}(t)\boldsymbol{\Psi}(t), \tag{A.9}$$

$$\mathbf{R}(t) = [2 - \lambda_1(t)]f_{\mathbf{F_I}}(t) + \frac{\lambda_2^2(t)}{\lambda_1(t)}f_{\mathbf{F_I}}(t)f_{\mathbf{F_P}}^2(t) +$$

$$+ \lambda_2(t)f_{\mathbf{F_P}}^2(t) + 2\frac{\lambda_2(t)}{\lambda_1(t)}f_{\mathbf{F_I}}(t)f_{\mathbf{F_P}}(t) + 2f_{\mathbf{F_P}}(t). \tag{A.10}$$

$$\square$$

Appendix B. Algorithms Analysis. The Stochastic Case - Perfect Matching

There are two sources of measurement noise, one acting on the primary transducer which gives the correlated measurement with the disturbance and the second acting on the measurement of the residual error (force, acceleration). For the primary transducer, the effect of the measurement noise is negligible since the signal to noise ratio is very high. The situation is different for the residual error where the effect of the noise can not be neglected.

In the presence of the measurement noise ($n(t)$), the equation of the a posteriori residual error becomes

$$\nu(t+1) = H(q^{-1})\left[\boldsymbol{\Theta} - \hat{\boldsymbol{\Theta}}(t+1)\right]^T \boldsymbol{\Psi}(t) + V(q^{-1})n(t+1). \tag{B.1}$$

The O.D.E. method [7] can be used to analyse the asymptotic behavior of the algorithm in the presence of noise. Taking into account the form of equation (B.1), one can directly use [14, Theorem 4.1] or [25, Theorem B1].

The following assumptions will be made:

1. $\lambda_1(t) = 1$ and $\lambda_2(t) = \lambda_2 > 0$;
2. $\hat{\boldsymbol{\Theta}}(t)$ generated by the algorithm belongs infinitely often to the domain D_S:

$$D_S \triangleq \{\hat{\boldsymbol{\Theta}} : \hat{P}(z^{-1}) = 0 \Rightarrow |z| < 1\}$$

   for which stationary processes

$$\boldsymbol{\Psi}(t, \hat{\boldsymbol{\Theta}}) \triangleq \boldsymbol{\Psi}(t)|_{\hat{\boldsymbol{\Theta}}(t)=\hat{\boldsymbol{\Theta}}=const}$$

$$\nu(t, \hat{\boldsymbol{\Theta}}) = \nu(t)|_{\hat{\boldsymbol{\Theta}}(t)=\hat{\boldsymbol{\Theta}}=const}$$

   can be defined;
3. $n(t)$ is a zero mean stochastic process with finite moments and independent of the sequence $w(t)$.

From (B.1) for $\hat{\Theta}(t) = \hat{\Theta}$, one gets

$$\nu(t+1, \hat{\Theta}) = H(q^{-1})\left[\Theta - \hat{\Theta}\right]^T \Psi(t, \hat{\Theta}) + V(q^{-1})n(t+1). \tag{B.2}$$

Since $\Psi(t, \hat{\Theta})$ depends upon $w(t)$ only, one concludes that $\Psi(t, \hat{\Theta})$ and $n(t+1)$ are independent. Therefore, using [14, Theorem 4.1] it results that if

$$H'(z^{-1}) = \frac{A_M A_G A_K}{P_{fb-ff}} \frac{GV}{L} - \frac{\lambda_2}{2} \tag{B.3}$$

is a SPR transfer function, one has $Prob\{\lim_{t\to\infty} \hat{\Theta}(t) \in D_C\} = 1$, where $D_C = \{\hat{\Theta} : \Psi^T(t, \hat{\Theta})(\Theta - \hat{\Theta}) = 0\}$. If furthermore $\Psi^T(t, \hat{\Theta})(\Theta - \hat{\Theta}) = 0$ has a unique solution (richness condition), the condition that $H'(z^{-1})$ be SPR implies that $Prob\{\lim_{t\to\infty} \hat{\Theta}(t) = \Theta\} = 1$.

Appendix C. Proof of Theorem 2

Proof. One needs first the following result:

Lemma 2. *Given the discrete transfer function*

$$H(z^{-1}) = \frac{B(z^{-1})}{A(z^{-1})} = \frac{b_0 + b_1 z^{-1} + \ldots + b_{n_B} z^{-n_B}}{1 + a_1 z^{-1} + \ldots + a_{n_A} z^{-n_A}}, \tag{C.1}$$

under the hypothesis:

H5) $H(z^{-1})$ *has all its zeros inside the unit circle,*
H6) $b_0 \neq 0$,

there exists a positive scalar gain K such that $\frac{H}{1+KH}$ is SPR.

Proof of Lemma 2. To analyse the strict positive realness of this transfer function, one has to check first that it's real part is strictly positive. We then have:

$$\text{Re}\{\frac{H(z^{-1})}{1 + K \cdot H(z^{-1})}\} = \frac{K \cdot \text{Re}\{H\}^2 + \text{Re}\{H\} + K \cdot \text{Im}\{H\}^2}{(1 + K \cdot \text{Re}\{H\})^2 + (K \cdot \text{Im}\{H\})^2}. \tag{C.2}$$

In eq. (C.2), the denominator is always strictly positive. Thus, the strict positive realness is satisfied if K is chosen such that the numerator of eq. (C.2) is also strictly positive. This is always true if K satisfies the relation

$$K > -\frac{\text{Re}\{H(e^{-j\omega})\}}{\text{Re}\{H(e^{-j\omega})\}^2 + \text{Im}\{H(e^{-j\omega})\}^2}, \quad 0 \leq \omega \leq \pi \cdot f_S,$$

f_S being the sampling frequency.

Next, the stability of $H/(1 + KH)$ is analyzed. Under hypothesis H6, the poles of $H/(1 + KH)$ are given by the roots of the polynomial

$$P(q^{-1}) = 1 + \frac{\sum_{p=1}^{n_A} a_p q^{-p} + K \sum_{m=1}^{n_B} b_m q^{-m}}{1 + Kb_0} \tag{C.3}$$

and assuming K large enough such that $Kb_m \gg a_p$,
$\forall m \in \{1, \ldots, n_B\}, p \in \{1, \ldots, n_A\}, P(q^{-1}) \cong$

$$\cong \begin{cases} 1 + \sum_{m=1}^{n_B} \frac{b_m}{b_0} q^{-m} & \text{if } n_B \geq n_A, \\ 1 + \sum_{m=1}^{n_B} \frac{b_m}{b_0} q^{-m} + \sum_{p=n_B+1}^{n_A} \frac{a_p}{1+Kb_0} q^{-p} & \text{if } n_B < n_A. \end{cases}$$

Thus for $n_B \geq n_A$, the poles and the zeros of $H/(1 + KH)$ become identical when $K \to \infty$. For $n_B < n_A$, in addition to the poles identical to the zeros of $B(q^{-1})$, $n_A - n_B$ poles appear that go to zero as $K \to \infty$. The hypothesis H5 has been introduced to assure the stability of the direct path when H6 is satisfied. Hypothesis H6 is necessary since if $b_0 = 0$, $H/(1 + KH)$ becomes unstable for large K. $\qquad \square$
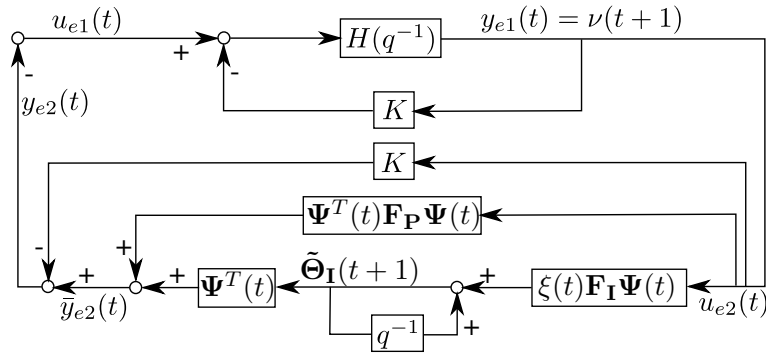

Figure C.14: Equivalent feedback representation of the PAA with "Integral + Proportional" adaptation with constant integral adaptation gain.

Using the above property, the EFR of the adaptive feedback system given by the eqs. (50) and (54) for $\lambda_2(t) \equiv 0$, $\lambda_1(t) \equiv 1$ (constant adaptation gain) can be represented as in Figure C.14, where K has been chosen such that $\frac{H}{1+KH}$ is SPR and

$$\tilde{\mathbf{\Theta}}_{\mathbf{I}}(t) = \hat{\mathbf{\Theta}}_{\mathbf{I}}(t) - \mathbf{\Theta}, \tag{C.4}$$

$$\nu(t+1) = -\frac{H(z^{-1})}{1 + KH(z^{-1})} y_{e2}(t), \tag{C.5}$$

$$\tilde{\mathbf{\Theta}}_{\mathbf{I}}(t+1) = \tilde{\mathbf{\Theta}}_{\mathbf{I}}(t) + \xi(t)\mathbf{F}_{\mathbf{I}}\mathbf{\Psi}(t)\nu(t+1), \tag{C.6}$$

$$y_{e2}(t) = \mathbf{\Psi}^T(t)\tilde{\mathbf{\Theta}}_{\mathbf{I}}(t) + (\mathbf{\Psi}^T(t)\mathbf{F}(t)\mathbf{\Psi}(t) - K)\nu(t+1), \tag{C.7}$$

$$u_{e2}(t) = \nu(t+1) \tag{C.8}$$

For the stability, it remains to show that the new equivalent feedback path is passive.

The proof is similar to that of [14, Theorem 3.3, pp. 109)] where Lemma 3.3 (pp. 110) is replaced by Lemma 2 of this paper. However, the details of the proof of Theorem 3.3 in [14] are not given. For the sake of completeness, the details of the proof of Theorem 2 are given next.

The proof is done by using [24, Theorem 1]. The adaptive system can be rearranged into the one given in Figure C.14. Under condition $T1$, the linear feedforward block from $u_{e1}(t)$ to $\nu(t+1)$ is SPR.

Given the choice in adaptation gain ($\lambda_2(t) \equiv 0$, $\lambda_1(t) \equiv 1$), the necessary condition for asymptotic stability is only that the time-varying feedback block belongs to the class $N(0)$ and, therefore, its input-

output product verifies Popov's inequality

$$\sum_{t=0}^{t_1} y_{e2}(t)u_{e2}(t) = \sum_{t=0}^{t_1} \bar{y}_{e2}(t)u_{e2}(t) - K\sum_{t=0}^{t_1} u_{e2}^2(t) \geq -\gamma_0^2. \tag{C.9}$$

It should be observed that with the current choice of $\lambda_2(t) \equiv 0$, $\lambda_1(t) \equiv 1$, one obtains $\xi(t) = 1$ from eq. (50h).

Taking into consideration eqs. (A.3) and (A.4)

$$\bar{y}_{e2}(t)u_{e2}(t) = \bar{y}_{e2}(t)\nu(t+1) = \tilde{\boldsymbol{\Theta}}_{\mathbf{I}}^T(t+1)\boldsymbol{\Psi}(t)\nu(t+1) +$$
$$+ \boldsymbol{\Psi}^T(t)\mathbf{F}_{\mathbf{P}}(t)\boldsymbol{\Psi}(t)\nu^2(t+1). \tag{C.10}$$

The first term in the right hand side can be further expressed as (see also Lemma 3.2 of [14])

$$\tilde{\boldsymbol{\Theta}}_{\mathbf{I}}^T(t+1)\boldsymbol{\Psi}(t)\nu(t+1) = \tilde{\boldsymbol{\Theta}}_{\mathbf{I}}^T(t+1)\mathbf{F_I}^{-1}\tilde{\boldsymbol{\Theta}}_{\mathbf{I}}(t+1) - \tilde{\boldsymbol{\Theta}}_{\mathbf{I}}^T(t+1)\mathbf{F_I}^{-1}\tilde{\boldsymbol{\Theta}}_{\mathbf{I}}(t). \tag{C.11}$$

On the other hand

$$[\tilde{\boldsymbol{\Theta}}_{\mathbf{I}}(t+1) - \tilde{\boldsymbol{\Theta}}_{\mathbf{I}}(t)]^T\mathbf{F_I}^{-1}[\tilde{\boldsymbol{\Theta}}_{\mathbf{I}}(t+1) - \tilde{\boldsymbol{\Theta}}_{\mathbf{I}}(t)] = \tilde{\boldsymbol{\Theta}}_{\mathbf{I}}^T(t+1)\mathbf{F_I}^{-1}\tilde{\boldsymbol{\Theta}}_{\mathbf{I}}(t+1) + \tilde{\boldsymbol{\Theta}}_{\mathbf{I}}^T(t)\mathbf{F_I}^{-1}\tilde{\boldsymbol{\Theta}}_{\mathbf{I}}(t) -$$
$$- 2\tilde{\boldsymbol{\Theta}}_{\mathbf{I}}^T(t+1)\mathbf{F_I}^{-1}\tilde{\boldsymbol{\Theta}}_{\mathbf{I}}(t) \geq 0, \tag{C.12}$$

from which, using (52) and (A.3), results

$$\tilde{\boldsymbol{\Theta}}_{\mathbf{I}}^T(t+1)\mathbf{F_I}^{-1}\tilde{\boldsymbol{\Theta}}_{\mathbf{I}}(t) = \frac{1}{2}\tilde{\boldsymbol{\Theta}}_{\mathbf{I}}^T(t+1)\mathbf{F_I}^{-1}\tilde{\boldsymbol{\Theta}}_{\mathbf{I}}(t+1) +$$
$$+ \frac{1}{2}\tilde{\boldsymbol{\Theta}}_{\mathbf{I}}^T(t)\mathbf{F_I}^{-1}\tilde{\boldsymbol{\Theta}}_{\mathbf{I}}(t) - \frac{1}{2}\boldsymbol{\Psi}^T(t)\mathbf{F_I}\boldsymbol{\Psi}(t)\nu^2(t+1). \tag{C.13}$$

Substituting the last equation back into (C.11) and using (52)

$$\tilde{\boldsymbol{\Theta}}_{\mathbf{I}}^T(t+1)\boldsymbol{\Psi}(t)\nu(t+1) = \frac{1}{2}\tilde{\boldsymbol{\Theta}}_{\mathbf{I}}^T(t+1)\mathbf{F_I}^{-1}\tilde{\boldsymbol{\Theta}}_{\mathbf{I}}(t+1) -$$
$$- \frac{1}{2}\tilde{\boldsymbol{\Theta}}_{\mathbf{I}}^T(t)\mathbf{F_I}^{-1}\tilde{\boldsymbol{\Theta}}_{\mathbf{I}}(t) + \frac{1}{2}\boldsymbol{\Psi}^T(t)\mathbf{F_I}\boldsymbol{\Psi}(t)\nu^2(t+1), \tag{C.14}$$

and summing up from $t = 0$ to t_1, one gets

$$\sum_{t=0}^{t_1} y_{e2}(t)\nu(t+1) = \frac{1}{2}\tilde{\boldsymbol{\Theta}}_{\mathbf{I}}^T(t_1+1)\mathbf{F_I}^{-1}\tilde{\boldsymbol{\Theta}}_{\mathbf{I}}(t_1+1) +$$
$$+ \sum_{t=0}^{t_1} \boldsymbol{\Psi}^T(t)\left(\frac{1}{2}\mathbf{F_I} + \mathbf{F_P}(t)\right)\boldsymbol{\Psi}(t)\nu^2(t+1) -$$
$$- K\sum_{t=0}^{t_1} \nu^2(t+1) - \frac{1}{2}\tilde{\boldsymbol{\Theta}}_{\mathbf{I}}^T(0)\mathbf{F_I}^{-1}\tilde{\boldsymbol{\Theta}}_{\mathbf{I}}(0). \tag{C.15}$$

From eq. (C.15) and the fact that $\mathbf{F_I}$ is positive definite, concludes that

$$\sum_{t=0}^{t_1} y_{e2}(t)u_{e2}(t) \geq -\frac{1}{2}\tilde{\boldsymbol{\Theta}}_{\mathbf{I}}^T(0)\mathbf{F_I}^{-1}\tilde{\boldsymbol{\Theta}}_{\mathbf{I}}(0) \tag{C.16}$$

as long as K satisfies condition $T2$ of the theorem, thus Popov's inequality is satisfied and the adaptive system is asymptotically stable. $\qquad\square$

Appendix D. Summary of Various Algorithms

Tables D.3 and D.4 give the details of various algorithms mentioned throughout the paper.

	Paper (Matrix gain)	Paper (Scalar gain)	[9] (Matrix gain)	[9] (Scalar gain)
Adap. gain	(50e)-(50g)	$\mathbf{F_I}(t)=\gamma(t)\mathbf{I}$ $\mathbf{F_P}(t)=\alpha(t)\mathbf{F_I}(t)$ $\mathbf{F}(t)=\mathbf{F_I}(t)+\mathbf{F_P}(t)$	(50e)-(50g) $\mathbf{F_P}=0$	$\mathbf{F_I}(t)=\gamma(t)\mathbf{I}$ $\mathbf{F}(t)=\mathbf{F_I}(t)$
$\lambda_2(t)$	$0\le\lambda_2(t)<2$	$=0$	$0\le\lambda_2(t)<2$	$=0$
$\lambda_1(t)$	$0<\lambda_1(t)\le1$	$0<\lambda_1(t)\le1$	$0<\lambda_1(t)\le1$	$0<\lambda_1(t)\le1$
$\xi(t)=$	$1+\frac{\lambda_2(t)}{\lambda_1(t)}\mathbf{\Psi}^T(t)\mathbf{F_P}(t)\mathbf{\Psi}(t)$	1	1	1
Prop. gain	$\alpha(t)>-0.5$	$\alpha(t)>-0.5$	$\alpha(t)=0$	$\alpha(t)=0$
$\nu(t+1)=$	$\varepsilon(t+1)+B_V^*\varepsilon(t)-$ $-A_V^*\nu(t)$	$\varepsilon(t+1)+B_V^*\varepsilon(t)-$ $-A_V^*\nu(t)$	$\varepsilon(t+1)$	$\varepsilon(t+1)$
$\varepsilon(t+1)=$	$\frac{\varepsilon^0(t+1)}{1+\mathbf{\Psi}^T(t)\mathbf{F}(t)\mathbf{\Psi}(t)}$			
$\mathbf{\Psi}(t)=$	$L\mathbf{\Phi}(t)$ $L_{I_L}=\hat{G};\ L_{II_L}=\frac{\hat{G}}{1+\hat{G}K};\ L_{III_L}=\frac{\hat{A}_M\hat{A}_G A_K}{\hat{P}_{fb-ff}}\hat{G}$ $\hat{P}_{fb-ff}=\hat{A}_M\hat{S}\left[\hat{A}_G A_K+\hat{B}_G B_K\right]-\hat{B}_M\hat{R}A_K\hat{A}_G$		$L\mathbf{\Phi}(t)$ $L_2=\hat{G};\ L_3=\frac{\hat{A}_M}{\hat{P}}\hat{G}$ $\hat{P}=\hat{A}_M\hat{S}-\hat{B}_M\hat{R}$	
$K=\frac{B_K}{A_K}$	$B_K=b_1^K z^{-1}+\ldots,\quad A_K=1+a_1^K z^{-1}+\ldots$		$B_K=0,\quad A_K=1$	
$G=\frac{B_G}{A_G}$	$B_G=b_1^G z^{-1}+\ldots,\quad A_G=1+a_1^G z^{-1}+\ldots$			
$M=\frac{B_M}{A_M}$	$B_M=b_1^M z^{-1}+\ldots,\quad A_M=1+a_1^M z^{-1}+\ldots$			

Table D.3: Comparison of algorithms for adaptive feedforward compensation in AVC with mechanical coupling.

	SHARF [16]	[8] (Scalar gain)	FULMS (Scalar gain)	[17]
Adap. gain	$\mathbf{F_I}=\gamma\mathbf{I},\ \mathbf{F_P}=0$ $\mathbf{F}=\mathbf{F_I}$	$\mathbf{F_I}=\gamma\mathbf{I},\ \mathbf{F_P}=0$ $\mathbf{F}=\mathbf{F_I}$	$\mathbf{F_I}(t)=\gamma(t)\mathbf{I}$ $\mathbf{F}(t)=\mathbf{F_I}(t)$	(50e)-(50g) $\mathbf{F_P}=0$
$\lambda_2(t)$	$=0$	$=0$	$=0$	$0\le\lambda_2(t)<2$
$\lambda_1(t)$	$=1$	$=1$	$0<\lambda_1(t)\le1$	$0<\lambda_1(t)\le1$
$\xi(t)=$	1	1	1	1
Prop. gain	$\alpha(t)=0$	$\alpha(t)=0$	$\alpha(t)=0$	$\alpha(t)=0$
$\nu(t+1)=$	$\varepsilon(t+1)+B_V^*\varepsilon(t)$	$\varepsilon(t+1)$	$\varepsilon(t+1)$	$\varepsilon^0(t+1)+B_V^*\varepsilon(t)$
$\varepsilon(t+1)=$	ε^0	$\frac{\varepsilon^0(t+1)}{1+\mathbf{\Psi}^T(t)\mathbf{F_I}(t)\mathbf{\Psi}(t)}$	ε^0	$\frac{\varepsilon^0(t+1)}{1+\mathbf{\Psi}^T(t)\mathbf{F}(t)\mathbf{\Psi}(t)}$
$\mathbf{\Psi}(t)=$	$\mathbf{\Phi}(t)$	$\mathbf{\Phi}(t)$	$L\mathbf{\Phi}(t),\quad L=\hat{G}$	$L\mathbf{\Phi}(t),\quad L=\hat{G}$
$K=\frac{B_K}{A_K}$	$B_K=0,\quad A_K=1$			
$G=\frac{B_G}{A_G}$	$B_G=b_1^G z^{-1}+\ldots$ $A_G=1+a_1^G z^{-1}+\ldots$	$B_G=1,\quad A_G=1$ or $G=SPR$	$B_G=b_1^G z^{-1}+\ldots$ $A_G=1+a_1^G z^{-1}+\ldots$	
$M=\frac{B_M}{A_M}$	$B_M=0,\quad A_M=1$	$B_M=b_1^M z^{-1}+\ldots,\quad A_M=1$		$B_M=0,\quad A_M=1$

Table D.4: Comparison of algorithms for adaptive feedforward compensation in AVC with mechanical coupling.

List of Figures

References

[1] S. Elliott, P. Nelson, Active noise control, Noise / News International (1994) 75–98.

[2] S. Elliott, T. Sutton, Performance of feedforward and feedback systems for active control, Speech and Audio Processing, IEEE Transactions on 4 (3) (1996) 214 –223.

[3] S. Kuo, D. Morgan, Active noise control: a tutorial review, Proceedings of the IEEE 87 (6) (1999) 943 – 973.

[4] J. Zeng, R. de Callafon, Recursive filter estimation for feedforward noise cancellation with acoustic coupling, Journal of Sound and Vibration 291 (3-5) (2006) 1061 – 1079.

[5] A. Wang, W. Ren, Convergence analysis of the filtered-u algorithm for active noise control, Signal Processing 83 (2003) 1239–1254.

[6] R. Fraanje, M. Verhaegen, N. Doelman, Convergence analysis of the filtered-u lms algorithm for active noise control in case perfect cancellation is not possible, Signal Processing 73 (1999) 255–266.

[7] L. Ljung, T. Söderström, Theory and practice of recursive identification, The M.I.T Press, Cambridge Massachusetts , London, England, 1983.

[8] C. Jacobson, J. Johnson, C.R., D. McCormick, W. Sethares, Stability of active noise control algorithms, Signal Processing Letters, IEEE 8 (3) (2001) 74 –76.

[9] I. Landau, M. Alma, T. Airimiţoaie, Adaptive feedforward compensation algorithms for active vibration control with mechanical coupling, Automatica 47 (10) (2011) 2185 – 2196.

[10] R. A. de Callafon, C. E. Kinney, Robust estimation and adaptive controller tuning for variance minimization in servo systems, Journal of Advanced Mechanical Design, Systems, and Manufacturing 4 (1) (2010) 130–142.

[11] L. Ray, J. Solbeck, A. Streeter, R. Collier, Hybrid feedforward-feedback active noise reduction for hearing protection and communication, The Journal of the Acoustical Society of America 120 (4) (2006) 2026–2036.

[12] E. Esmailzadeh, A. Alasty, A. Ohadi, Hybrid active noise control of a one-dimensional acoustic duct, Journal of vibration and acoustics 124 (1) (2002) 10–18.

[13] B. Anderson, R. Bitmead, C. Johnson, P. Kokotovic, R. Kosut, I. Mareels, L. Praly, B. Riedle, Stability of adaptive systems, The M.I.T Press, Cambridge Massachusetts , London, England, 1986.

[14] I. D. Landau, R. Lozano, M. M'Saad, A. Karimi, Adaptive control, 2nd Edition, Springer, London, 2011.

[15] M. Tomizuka, Parallel mras without compensation block, Automatic Control, IEEE Transactions on 27 (2) (1982) 505 – 506.

[16] M. Larimore, J. Treichler, J. Johnson, C., Sharf: An algorithm for adapting iir digital filters, Acoustics, Speech and Signal Processing, IEEE Transactions on 28 (4) (1980) 428 – 440.

[17] A. Montazeri, J. Poshtan, A new adaptive recursive rls-based fast-array iir filter for active noise and vibration control systems, Signal Processing 91 (1) (2011) 98 – 113.

[18] X. Sun, D.-S. Chen, A new infinte impulse response filter-based adaptive algorithm for active noise control, Journal of Sound and Vibration 258 (2) (2002) 385 – 397.

[19] X. Sun, G. Meng, Steiglitzmcbride type adaptive iir algorithm for active noise control, Journal of Sound and Vibration 273 (1-2) (2004) 441 – 450.

[20] G. Bierman, Factorization methods for discrete sequential estimation, Academic Press, New York, 1977.

[21] A. Montazeri, J. Poshtan, A computationally efficient adaptive iir solution to active noise and vibration control systems, IEEE Trans. on Automatic Control AC-55 (2010) 2671 – 2676.

[22] M. Alma, I. D. Landau, T.-B. Airimitoaie, Adaptive feedforward compensation algorithms for avc systems in the presence of a feedback controller, Automatica 48 (5) (2012) 982 – 985.

[23] I. Landau, An extension of a stability theorem applicable to adaptive control, Automatic Control, IEEE Transactions on 25 (4) (1980) 814 – 817.

[24] I. Landau, H. Silveira, A stability theorem with applications to adaptive control, Automatic Control, IEEE Transactions on 24 (2) (1979) 305 – 312.

[25] I. Landau, A. Karimi, Recursive algorithms for identification in closed loop. a unified approach and evaluation, Automatica 33 (8) (1997) 1499–1523.

[26] I. Landau, A. Karimi, A. Constantinescu, Direct controller order reduction by identification in closed loop, Automatica 37 (2001) 1689–1702.

[27] I. Landau, A. Constantinescu, P. Loubat, D. Rey, A. Franco, A methodology for the design of feedback active vibration control systems, in: Proceedings of the European Control Conference, Porto, Portugal, 2001, pp. 1571–1576.

[28] I. Landau, J. Langer, D. Rey, J. Barnier, Robust control of a 360 flexible arm using the combined pole placement/sensitivity function shaping method, IEEE Transactions on Control Systems Technology 4(4) (1996) 369–383.